N7172278

A THEORETICAL INVESTIGATION OF THE INFLUENCE OF THE NATURAL FREQUENCY OF A SECOND-ORDER AUTOPILOT UPON THE DYNAMIC PERFORMANCE CHARACTERISTICS OF AN ATTITUDE-ANGLE CONTROL SYSTEM WITH A RATE-DAMPED SUPERSONIC MISSILE CONFIGURATION

1953

Declassified
Hdq Ltr. 10/8/5.
File E32-18
E26-1013
[redacted]

A THEORETICAL INVESTIGATION OF THE INFLUENCE OF THE NATURAL FREQUENCY OF A SECOND-ORDER AUTOPILOT UPON THE DYNAMIC PERFORMANCE CHARACTERISTICS OF AN ATTITUDE-ANGLE CONTROL SYSTEM WITH A RATE-DAMPED SUPERSONIC MISSILE CONFIGURATION

A Thesis

Presented to

the Faculty of the Department of Engineering

University of Virginia

APR 1971
RECEIVED

Reproduced from best available copy.

In Partial Fulfillment

of the Requirements for the Degree

Master of Electrical Engineering

Anthony L. Passera

1953

78

DECLASSIFIED
CONFIDENTIAL
SECURITY INFORMATION

APPROVAL SHEET

This thesis is submitted in partial fulfillment of
the requirements for the degree of
Master of Electrical Engineering

Author

Approved:

Faculty Advisor

For Subcommittee

Chairman, Committee on Graduate Studies
in Engineering

1953
DECLASSIFIED
CONFIDENTIAL

DECLASSIFIED
CONFIDENTIAL
SECURITY INFORMATION

TABLE OF CONTENTS

CHAPTER	PAGE
I. INTRODUCTION	1
Types and purpose for controls	1
Statement of the problem and previous work done	3
Statement of purpose	4
II. DESCRIPTION OF THE CONTROL SYSTEM	6
The supersonic missile	7
The rate gyro and servomotor combination .	8
The autopilot	10
III. THE ANALYSIS PROCEDURE	19
Adjustment of the static gains, K_r and K_A .	19
Method of obtaining the transient responses	22
IV. RESULTS AND DISCUSSION	24
Attitude-angle transient responses	29
Control-surface-deflection and normal-acceleration transient responses	39
V. CONCLUSIONS	51
BIBLIOGRAPHY	53
APPENDIX	56

DECLASSIFIED
CONFIDENTIAL

DECLASSIFIED
CONFIDENTIAL
SECURITY INFORMATION

LIST OF TABLES

TABLE PAGE

I. Missile Transfer Function Coefficients for Various Values of Mach Number and Altitude . . 17

II. Autopilot and Rate-Gyro-Servo Static Gains Tabulated against Autopilot Natural Frequency 25

DECLASSIFIED
CONFIDENTIAL

DECLASSIFIED

LIST OF FIGURES

FIGURE PAGE

1. Sketch of the Missile Configuration Illustrating Significant Flight Angles and Static Margin . . 2
2. Photograph of the Missile Configuration 9
3. Schematic Diagram of the Rate Gyro and Servomotor Combination 11
4. Photograph of the Rate Gyro and Servomotor Combination 12
5. Experimental Transient Response of the Rate Gyro and Servomotor Combination to a Unit Step $\dot{\theta}_o$, and the Frequency Response Determined by the Fourier Series 13
6. Schematic and Block Diagrams of a Possible Autopilot Arrangement Having a Second-Order Characteristic Equation 15
7. Representative Attitude-Angle Transient Response Illustrating Transient Characteristics: Amplitude of the Initial Overshoot, Response Time, Rise Time, and Transient Error 27
8. Longitudinal Transient Responses, $\theta_o(t)$, of the Control System to a Unit Step Input Signal Calling for a Change in Attitude of 1°. $K_r = 0.10$; $K_A = 1.26$ 30

DECLASSIFIED

DECLASSIFIED

FIGURE PAGE

9. Longitudinal Transient Responses, $\theta_o(t)$, of the Control System to a Unit Step Input Signal Calling for a Change in Attitude of 1°. $K_r = 0.16$; $K_A = 2.82$ 31

10. Longitudinal Transient Responses, $\theta_o(t)$, of the Control System to a Unit Step Input Signal Calling for a Change in Attitude of 1°. $K_r = 0.13$; $K_A = 2.43$ 32

11. Longitudinal Transient Responses, $\theta_o(t)$, of the Control System to a Unit Step Input Signal Calling for a Change in Attitude of 1°. $K_r = 0.08$; $K_A = 2.32$ 33

12. Attitude-Angle Transient Characteristics, Response Time and Rise Time, Plotted against Autopilot Natural Frequency. ζ of Autopilot, 0.5 34

13. Plot of $\int|\varepsilon_1(t)|dt$ for the Rate-Damped Missile and Autopilot Combination against Autopilot Natural Frequency in Response to a Step θ_i. ζ of Autopilot, 0.5 35

14. Frequency Responses of the Control System for an Autopilot Natural Frequency of 50 Radians per Second. $K_r = 0.16$; $K_A = 2.82$; $M = 2.0$; Altitude = 4,000 Feet 38

DECLASSIFIED

DECLASSIFIED
CONFIDENTIAL
SECURITY INFORMATION

FIGURE PAGE

15. Longitudinal Transient Responses, $\delta(t)$, of the Control System to a Unit Step Input Signal Calling for a Change in Attitude of 1°. $K_r = 0.10$; $K_A = 1.26$ 40

16. Longitudinal Transient Responses, $\delta(t)$, of the Control System to a Unit Step Input Signal Calling for a Change in Attitude of 1°. $K_r = 0.16$; $K_A = 2.82$ 41

17. Longitudinal Transient Responses, $\delta(t)$, of the Control System to a Unit Step Input Signal Calling for a Change in Attitude of 1°. $K_r = 0.13$; $K_A = 2.43$ 42

18. Longitudinal Transient Responses, $\delta(t)$, of the Control System to a Unit Step Input Signal Calling for a Change in Attitude of 1°. $K_r = 0.08$; $K_A = 2.32$ 43

19. Longitudinal Transient Responses for Normal Acceleration, $n(t)$, of the Control System to a Unit Step Input Signal Calling for a Change in Attitude of 1°. $K_r = 0.16$; $K_A = 2.82$ 44

DECLASSIFIED
CONFIDENTIAL

DECLASSIFIED

FIGURE PAGE

20. Longitudinal Transient Responses for Normal Acceleration, n(t), of the Control System to a Unit Step Input Signal Calling for a Change in Attitude of 1°. M = 2.0; Altitude, 4,000 Feet; ζ of Autopilot, 0.5 45

21. Plot of Total δ Travel against Autopilot Natural Frequency in Response to a Step Input Signal. ζ of Autopilot, 0.5 47

22. Plot of $n(t)_{max}$ against Autopilot Natural Frequency in Response to a Step Input Signal. M = 2.0; Altitude, 4,000 Feet 50

DECLASSIFIED

DECLASSIFIED

DEFINITION OF SYMBOLS

d missile's static margin

i solenoid current, milliamps

K static gain constant of the missile, $\frac{\dot{\theta}_o}{\delta}$, degrees/second per degree

K_A static gain constant of the autopilot, $\frac{\delta_A}{\epsilon_1}$, degrees per volt

K_g static gain constant of the missile, $\frac{n}{\dot{\theta}_o}$, g's per degree/second

K_o static gain constant of the amplifier and solenoid, milliamps per volt

K_r static gain constant of the rate gyro and servomotor combination, $\frac{\delta_r}{\dot{\theta}_o}$, degrees per degree/second

K_1 proportionality constant between the transfer valve linear displacement and solenoid current, $\frac{y}{i}$, inches per milliamp

K_2 proportionality constant between the servomotor output velocity and the transfer valve linear displacement, $\frac{\dot{x}}{y}$, inches/second per inch

K_3 proportionality constant between the feedback voltage and the servomotor linear displacement, $\frac{\epsilon_2}{x}$, volts per inch

M Mach number, nondimensionalized constant

DECLASSIFIED

n nondimensionalized normal acceleration of the missile, g's

s Laplace transform variable corresponding to the differential operator, $D \triangleq \frac{d}{dt}$

x servomotor linear displacement, inches

y transfer valve linear displacement, inches

α missile angle of attack, degrees

γ missile flight-path angle, degrees

δ control-surface deflection of the missile, $\delta_A - \delta_r$, degrees

δ_A control-surface-deflection output of the autopilot, degrees

δ_r control-surface-deflection output of the rate gyro and servomotor combination, degrees

ζ quadratic damping ratio of the autopilot, nondimensionalized constant

ζ_1 quadratic damping ratio of the missile, nondimensionalized constant

ϵ autopilot error signal, $\epsilon_1 - \epsilon_2$, volts

ϵ_1 control system error signal sensed by the autopilot free gyro, $\theta_1 - \theta_o$, volts

ϵ_2 autopilot feedback voltage proportional to the servomotor linear displacement, volts

DECLASSIFIED

θ_i input attitude command signal measured from some reference or uncaged autopilot gyro position, degrees

θ_o output attitude angle measured from the same reference as θ_i, degrees

τ time constant of the missile's linear factor, seconds

τ_o time constant of the amplifier and solenoid, seconds

ϕ missile's roll angle

ω_n undamped natural frequency of the autopilot, radians per second

ω_{n_1} undamped natural frequency of the missile, radians per second

DECLASSIFIED

DECLASSIFIED

CHAPTER I

INTRODUCTION

Types and purpose for controls. The general research program of automatic control and stabilization at the Pilotless Aircraft Research Division of the Langley Aeronautical Laboratory is concerned with the dynamic performance characteristics of an automatically controlled supersonic missile configuration. This controlled missile, or control system, may be combined with a missile guidance system such as an infrared, acoustic, or radar-operated seeker so that the combination of the control system and the guidance system will be able to seek out and collide with a moving or stationary target. The form of these targets may vary from a high-speed maneuverable jet aircraft to a strategic ground installation such as a factory. A seeker built into the nose of a high-performance supersonic missile configuration will give the necessary command signals with some dynamic error--error in the dynamic state; the control system must respond to these signals with sufficient accuracy to cause a collision with a desired target.

Some types of controls that may be used alone or in a combination of two or more are attitude angle, flight path angle, normal acceleration, and roll angle. The significant flight angles are illustrated in Figure 1.

DECLASSIFIED

CONFIDENTIAL

CONFIDENTIAL
SECURITY INFORMATION

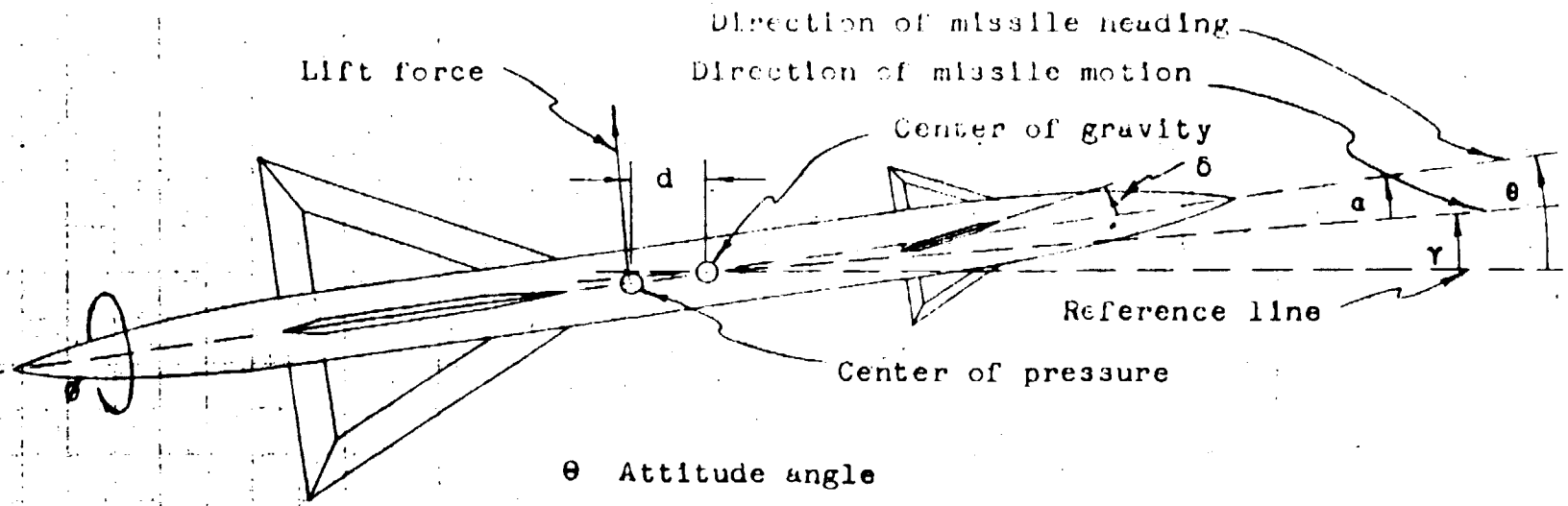

θ Attitude angle

α Angle of attack

γ Flight-path angle

Ø Roll angle

d Static margin

δ Control-surface deflection

Figure 1.- Sketch of the missile configuration illustrating significant flight angles and static margin.

CONFIDENTIAL

DECLASSIFIED
DECLASSIFIED

Statement of the problem and previous work done. In this paper, a theoretical investigation was made of the influence of the autopilot natural frequency upon the attitude control system--a control of the missile's heading during flight. The accuracy of the control system, or the ability of the output to follow the input command signal with little dynamic error, will improve as any of the control system elements, such as the autopilot, in the forward circuit approaches a simple proportional control with no dynamics in the element's transfer function. This element would have a large pass band of frequencies where the amplitude ratio is constant, and the phase lag is zero. If this same element operates on the outer-loop error signal, a step input command signal to the control system will cause an almost-instantaneous response requiring extremely high time rates of change of signal at the element's output. For this reason, it is not always advantageous to have such a perfect element follow the error signal since the power and energy output required is not practical with servomotors and associated gear available at the present time. Also, the cost of these servomotors and associated gear becomes excessive as the pass band required becomes large; therefore limiting the pass band of a servomechanism element operating on the outer-loop error signal to a point where there is no appreciable impairment of the system's accuracy is usually

DECLASSIFIED

DECLASSIFIED
DECLASSIFIED

desirable.

As a result of work done in an earlier paper, the accuracy of control was improved by the addition of rate feedback to the transfer function of a small-static-margin missile.[1] Rate feedback increases the damping ratio and the undamped natural frequency of the quadratic factor or characteristic equation of the missile's transfer function. In this same paper, a perfect proportional autopilot was the error-sensing device of a zero steady-state error position servomechanism. A perfect proportional autopilot is one that has a ratio of output to input equal to a constant, K, for all possible frequencies. The study herein considers the addition of dynamics in the form of a second-order characteristic equation to the autopilot transfer function. Now, instead of the ratio of output to input being a constant, K, for all possible frequencies, this ratio is now a complex function of frequency having an amplitude as well as a phase response. The rate feedback element is a rate gyro and servomotor combination designed and tested by the Control Laboratory at Langley.

Statement of purpose. The purpose of this paper is

---

[1] Walter C. Nelson and Anthony L. Passera, A Theoretical Investigation of the Influence of Auxiliary Damping in Pitch on the Dynamic Characteristics of a Proportionally Controlled Supersonic Missile Configuration, NACA RM L50F30, 1950.

DECLASSIFIED
CONFIDENTIAL

DECLASSIFIED

to investigate the effects of the autopilot natural frequency upon the attitude control system in terms of the transient characteristics, and to determine how low the natural frequency should be in order to yield a realizable system with respect to cost and with respect to accumulator energy and power requirements without too much loss in control accuracy over a Mach number and altitude range. The results of this investigation are presented in the form of attitude-angle, control-surface-deflection, and normal-acceleration transient responses in response to a unit step input command signal for several flight conditions.

DECLASSIFIED

UNCLASSIFIED
CLASSIFIED

CHAPTER II

DESCRIPTION OF THE CONTROL SYSTEM

The attitude control system consists of a supersonic missile, a rate gyro and servomotor combination, and an autopilot. This control system controls the heading of the missile during flight. The input signal, θ_i, is a desired heading required by a guidance system and is measured from the uncaged position of a free gyro rotor axis. The guidance system continuously performs the functions of "seeing" a target and computing what changes in the value of the existing input, θ_i, are required to cause a collision with the target. The rotor of the gyro holds its space reference during flight so that the output angle, θ_o, is formed by the axis of the gyro rotor and the missile heading. A wire-wound pickoff supplies a voltage proportional to this angle and the amplifier of the autopilot responds to the error signal, $\theta_i - \theta_o$.

To sum up this discussion, a guidance system calls for a particular heading, the free gyro compares the existing missile heading with the heading required by the guidance system producing an error voltage. The control system responds to this error voltage correcting the output, θ_o, so it agrees with the input, θ_i. There is no steady-state error voltage in this system since a constant voltage ϵ_1

UNCLASSIFIED

would always produce a time rate of change of θ_o, and not merely θ_o itself. This means that the output would eventually become equal to the input after some passing of time.

The supersonic missile. The missile considered in this paper is a symmetrical cruciform configuration shown in Figure 2. A flight test of this configuration is reported in a paper by Gardiner and Zarovsky.[1] The wings and canard fins are of delta design with the leading edges swept back 60° and have modified-double-wedge cross sections. The fuselage fineness ratio is 16. The canard fins provide the required longitudinal control while the auxiliary damping is provided through these same canard fins by the action of a rate gyro and servomotor combination.

The transfer function of the missile is obtained by summing up the moments about an axis through the center of gravity and perpendicular to the missile heading, and by summing the lift forces. The coefficients for the transfer function are experimentally determined by flight testing the missile at Wallops Island in Virginia. The missile control surfaces or canards are pulsed during flight while the response of the missile to these pulses is telemetered to a ground station and the results recorded. The missile

1 Robert A. Gardiner and Jacob Zarovsky, Rocket-Powered Flight Test of a Roll-Stabilized Supersonic Missile Configuration, NACA RM L9K01a, 1950.

DECLASSIFIED

has sufficient instrumentation so that the telemetered results, after the necessary computations are made, will yield the stability derivatives. The transfer function coefficients can then be determined from these stability derivatives.

The canard fins are the forward control surfaces shown in Figure 2. The angular deflection of these control surfaces are the result of the combined outputs of the autopilot, and the rate gyro and servomotor combination taken with regard to their proper signs. Four canard fins are indicated by the figure. These four may be employed to control the missile heading in space if the missile is prevented from rolling over by means of a roll control system. Such a roll control system indicates errors in roll position and is a servomechanism for correcting the errors by actuating wing-tip control surfaces on the aft section of the missile. Diametrically opposite canard fins are controlled as one control surface to provide the required missile heading in one plane.

The rate gyro and servomotor combination. The rate gyro and servomotor combination gives additional damping to and increases the natural frequency of the quadratic factor in the missile's transfer function by providing a control-surface deflection proportional to the time rate of

DECLASSIFIED

DECLASSIFIED
CONFIDENTIAL
SECURITY INFORMATION

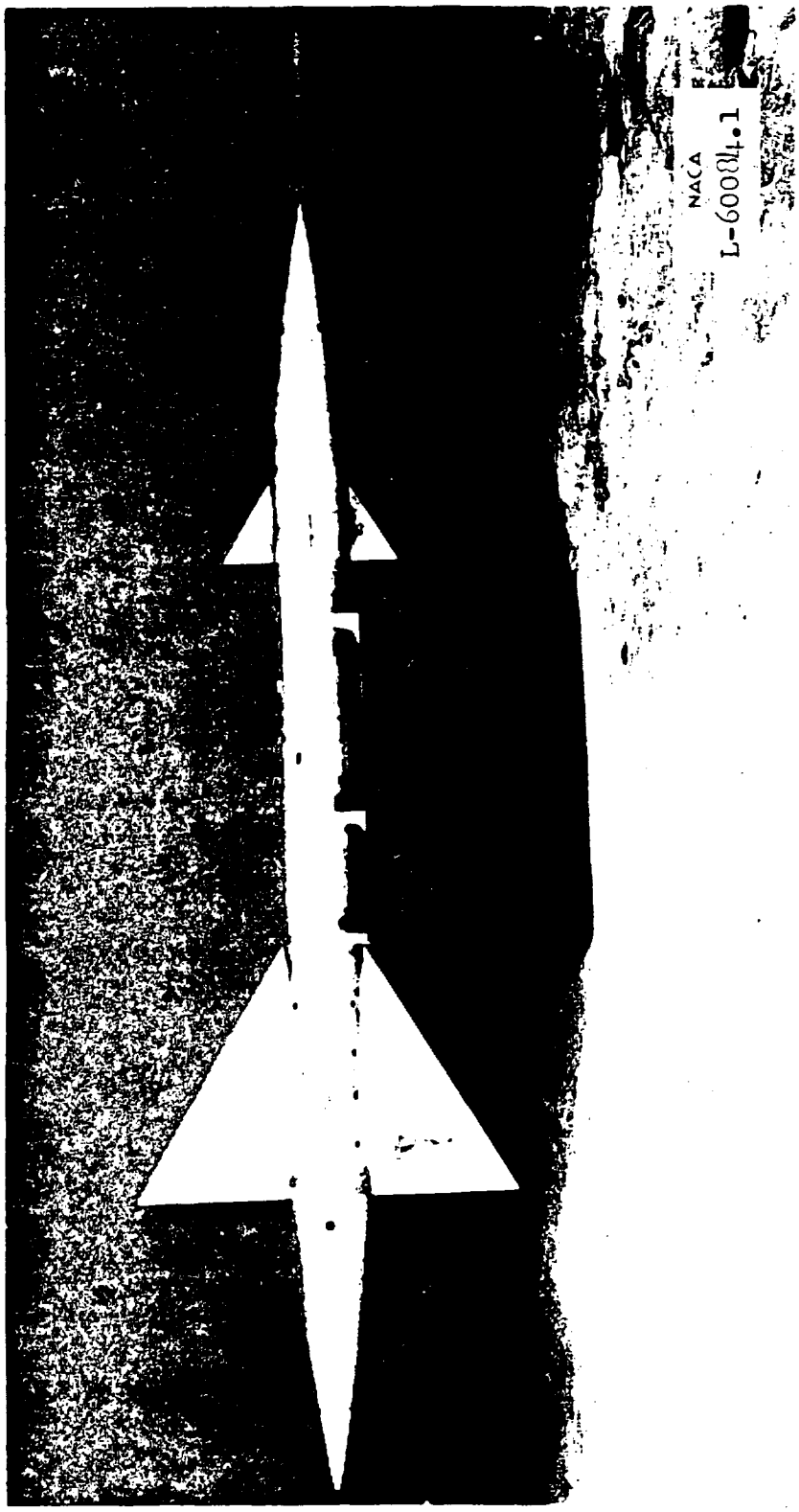

Figure 2.- Photograph of the missile configuration.

DECLASSIFIED
CONFIDENTIAL

change of the attitude angle. Figures 3 and 4 illustrate the arrangement that yields the experimental response shown on Figure 5. The torque produced by the rate gyro, due to $\dot{\theta}_o$, is opposed by a spring so that any angular displacement of the gyro gimbal is proportional to $\dot{\theta}_o$. The valve controlling the flow of oil to the servomotor is linked directly to the rate gyro gimbal. This gimbal, in turn, has its motion damped by two dashpots linked in parallel. The transient response to a step $\dot{\theta}_o$ of the rate gyro and servomotor combination was obtained experimentally at the Langley Laboratory by causing a step deflection of the rate-sensitive gyro gimbal. Figure 5 shows the transient response obtained and the associated frequency response determined by the Fourier series.[2]

The autopilot. Four attitude-sensitive autopilots are considered in the analysis and approximated by the transfer function

$$\frac{\delta_A}{\epsilon_1}(s) = \frac{K_A \omega_n^2}{s^2 + 2\zeta\omega_n s + \omega_n^2}$$

with the following constant coefficients: $\omega_n = 30$, 50, 70, and 140 radians per second and $\zeta = 0.5$. The schematic and block diagrams of a possible autopilot arrangement yielding

[2] Robert C. Seamans, Benjamin G. Bromberg, and L. E. Payne, "Application of the Performance Operator to Aircraft Automatic Control", Journal of Aeronautical Science, 15:535-55, September, 1948.

CONFIDENTIAL
SECURITY INFORMATION

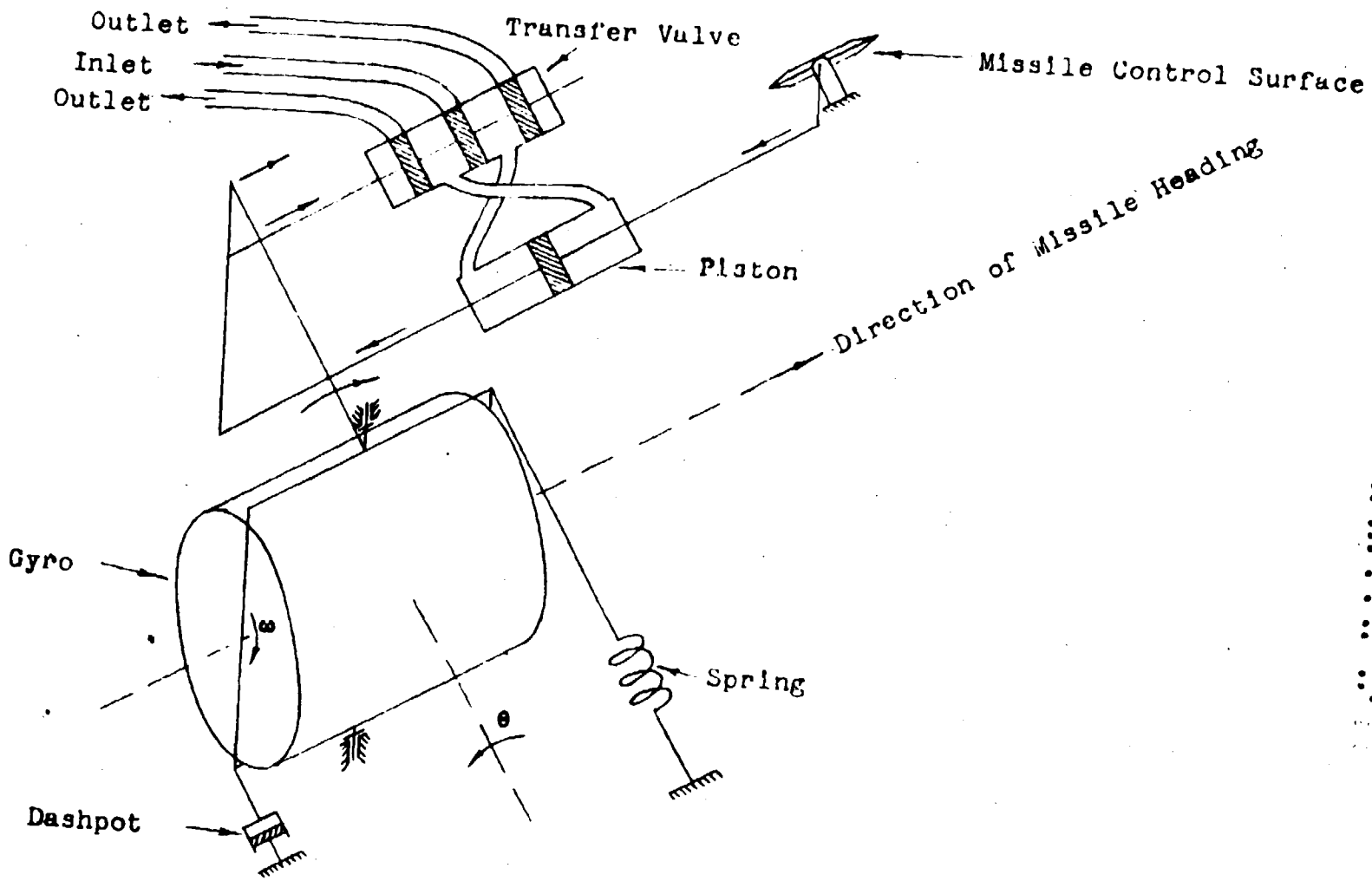

Figure 3.- Schematic diagram of the rate gyro and servomotor combination.

CONFIDENTIAL

CONFIDENTIAL
SECURITY INFORMATION

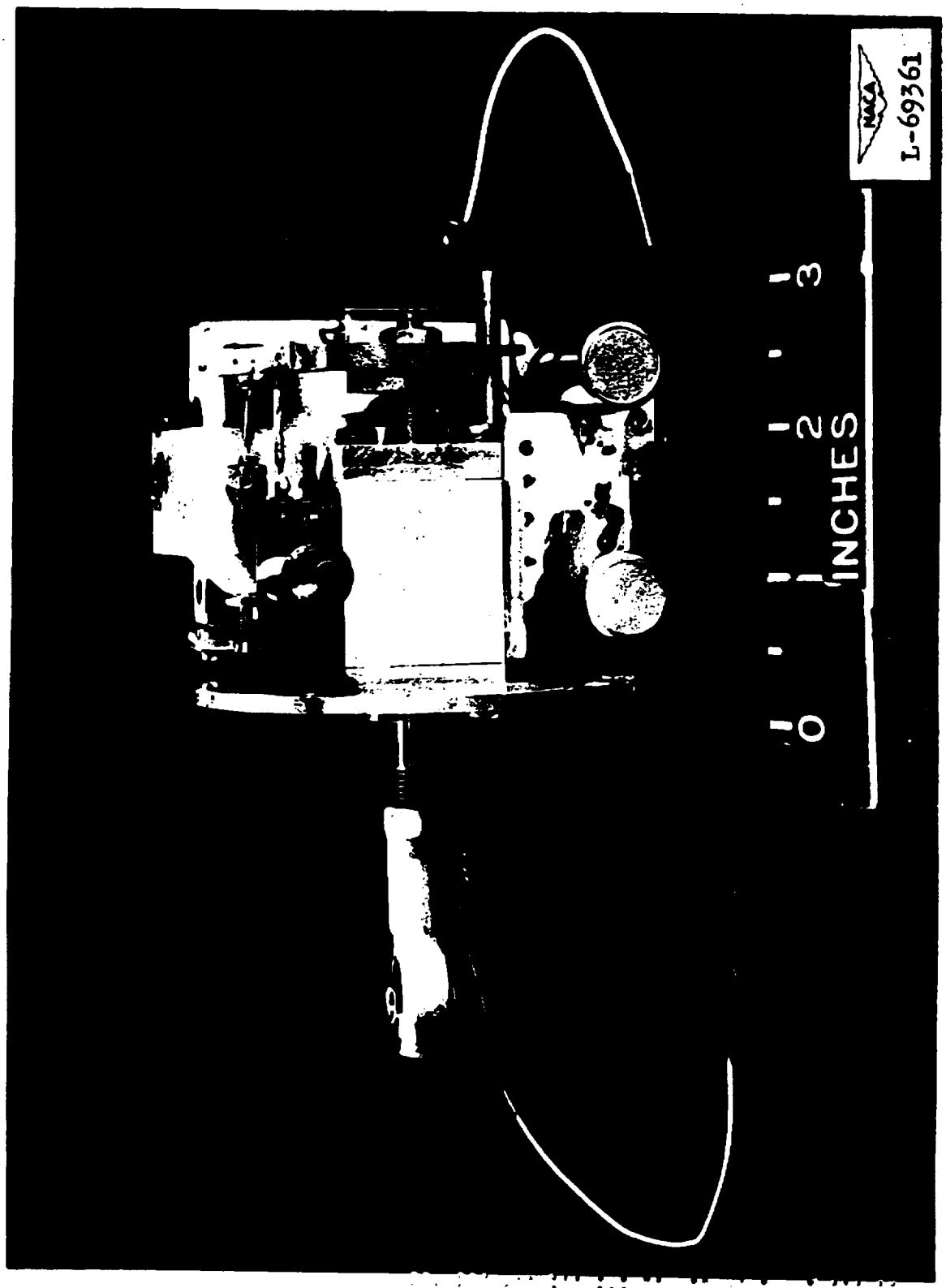

Figure 4.- Photograph of the rate gyro and servomotor combination.

CONFIDENTIAL

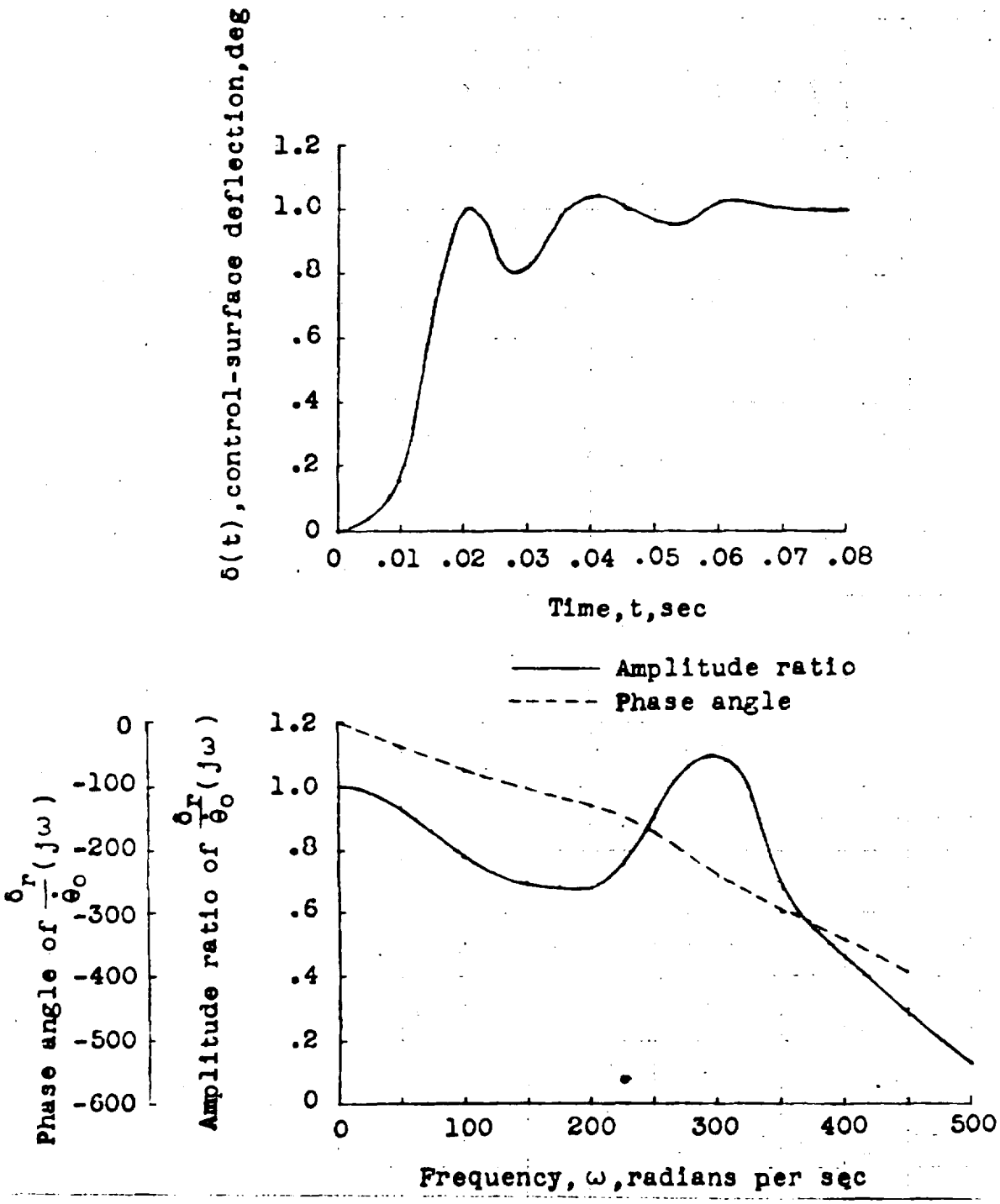

Figure 5.- Experimental transient response of the rate gyro and servomotor combination to a unit step $\dot{\theta}_o$, and the frequency response determined by the Fourier series.

this second-order characteristic equation is shown in Figure 6. This transfer function is valid only when the system is considered to be entirely linear or when the effects of saturation in the amplifier, mechanical stops on the servomotor travel, dead spot in the control valve flow characteristics, and other non-linearities are neglected. This is in keeping with linear servomechanism theory. The physical autopilot consists of a free gyro sensitive to attitude-angle error plus a servomechanism for deflecting the missile's control surfaces or canard fins. The value of the damping ratio chosen has proven from experience to be a good approximation of such a physical arrangement.

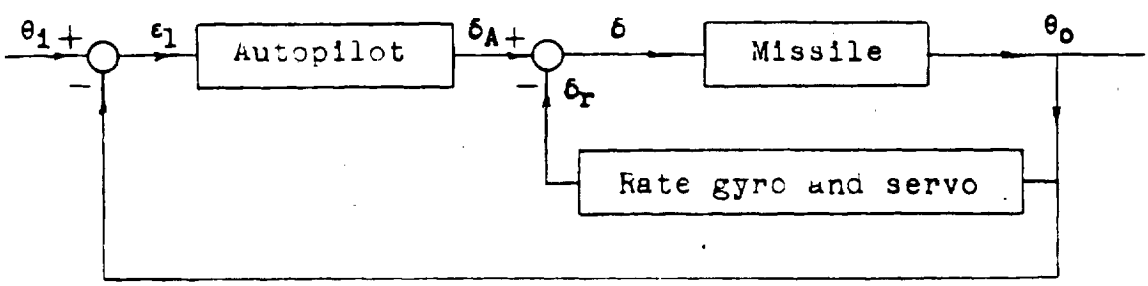

The following is a description of the attitude control system block diagram. An input signal or command, θ_i, calls for a change in attitude angle from some reference or uncaged position of the autopilot gyro. The error signal, ϵ_1, that causes the autopilot to respond is

$$\epsilon_1(s) = \theta_i(s) - \theta_o(s)$$

The autopilot responds to this signal and produces an

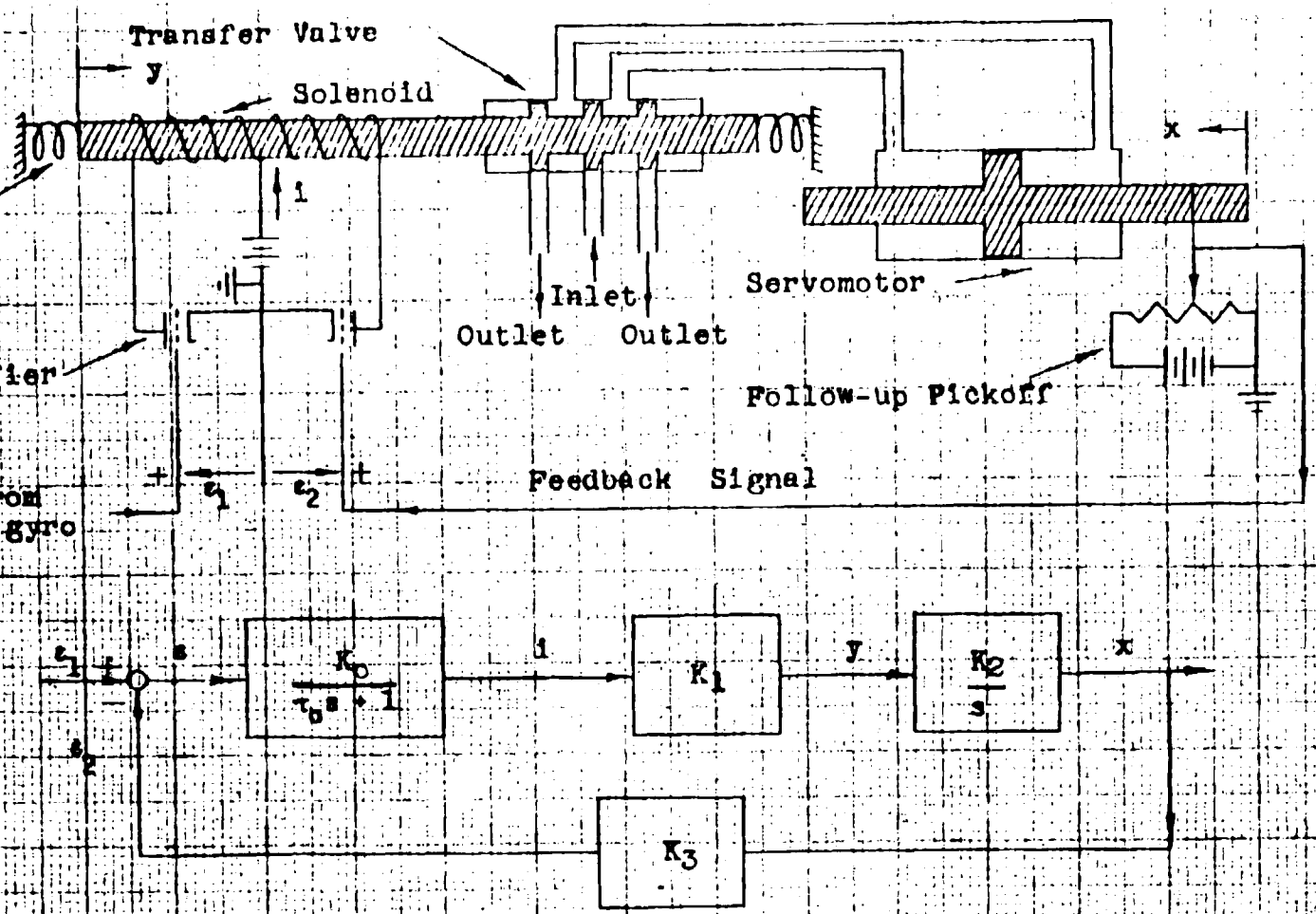

Figure 6.- Schematic and block diagrams of a possible autopilot arrangement having a second-order characteristic equation.

output that satisfies the transfer function

$$\frac{\delta_A}{\varepsilon_1}(s) = \frac{K_A \omega_n^2}{s^2 + 2\zeta\omega_n s + \omega_n^2}$$

The rate gyro and servomotor combination produces a control-surface deflection, δ_r, in response to the signal, $\dot{\theta}_o$. The transfer function for the rate gyro is not available in analytical form, but for this paper, an experimentally determined transient response was available. This control-surface deflection, $\delta = \delta_A - \delta_r$, causes the missile to respond and a change of pitch angle, θ_o, is produced according to the transfer function

$$\frac{\theta_o}{\delta}(s) = \frac{K(\tau s + 1)}{s(s^2 + 2\zeta_1\omega_{n_1} s + \omega_{n_1}^2)}$$

This transfer function is obtained from the linear differential equations of motion with constant coefficients by assuming two degrees of freedom longitudinally and disturbance from level flight. The Laplace transformation is applied to these equations with all initial conditions equated to zero, and then the equations solved for θ_o/δ. The magnitude of the missile's constant coefficients are functions of the flight conditions--Mach number and altitude--, and the resulting values of the coefficients are presented in Table I. These constant coefficients are expressed in terms of longitudinal stability derivatives in

TABLE I

MISSILE TRANSFER FUNCTION COEFFICIENTS FOR VARIOUS VALUES OF MACH NUMBER AND ALTITUDE

[Static margin, 2 inches at $M = 1.6$;

$$\frac{\theta_o}{\delta}(s) = \frac{K(\tau s + 1)}{s(s^2 + 2\zeta_1 \omega_{n_1} s + \omega_{n_1}^2)}]$$

Mach number	Altitude (feet)	K	τ	ζ_1	ω_{n_1}
1.6	4,000	1800	0.268	0.26	13.8
1.6	30,000	241	.687	.17	8.0
1.2	4,000	1240	.287	.21	13.5
2.0	4,000	3250	.213	.37	11.8

a recent paper written by Seaberg and Smith.[3]

The normal-acceleration transient response to a unit step input, $n(t)$, was obtained by cascading another transfer function onto the original attitude-angle block diagram.

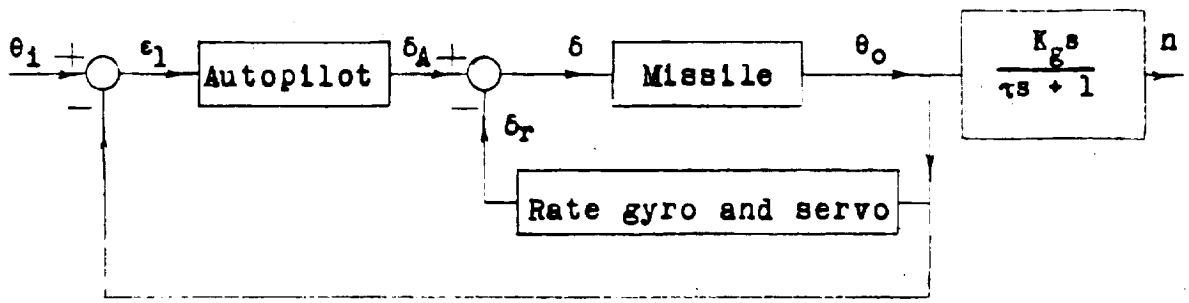

The operational form indicated for determining n is given by

$$n(s) = \frac{K_g s}{\tau s + 1}\,\theta_o(s)$$

where K_g has the units, g's per degree/second.

Finally, the control-surface-deflection transient response to a unit step was obtained from the $\frac{\delta}{\theta_i}(s)$ response where

$$\frac{\delta}{\theta_i}(s) = \frac{\theta_o}{\theta_i}(s) \cdot \frac{\delta}{\theta_o}(s)$$

[3] Ernest C. Seaberg and Earl F. Smith, A Theoretical Investigation of an Automatic Control System with Primary Sensitivity to Normal Accelerations as Used to Control a Supersonic Canard Missile Configuration, NACA RM L51D23, 1951.

CHAPTER III

THE ANALYSIS PROCEDURE

Adjustment of the static gains, K_r and K_A. The method and procedure for obtaining the over-all $\frac{\theta_o}{\theta_i}(j\omega)$ frequency response by closing the two loops of the control-system block diagram was in accordance with linear servomechanism theory.[1] The static gains (zero-frequency amplitude ratios), K_r of the rate gyro and servomotor combination and K_A of a particular autopilot, were chosen to yield approximately a minimum-error response for one flight condition, that is, a response with $\int|\epsilon_1(t)|\,dt$ nearly minimum for a step input command signal, $\theta_i(t)$. Since an analytical method of error minimization was not available for this control system, plotting the control-system frequency response on the Nichols chart[2] was necessary; then the rate gyro and servomotor combination and autopilot static gains were adjusted graphically until the over-all closed-loop frequency response, $\frac{\theta_o}{\theta_i}(j\omega)$, closely represented the zero-decibel contour for as high a range of frequencies as possible. This was considered a good approximation of a

[1] Gordon S. Brown and Donald B. Campbell, Principles of Servomechanisms (New York: John Wiley and Sons, 1948).

[2] Harold Chestnut and Robert W. Mayer, Servomechanisms and Regulating System Design (New York: John Wiley and Sons, 1951), I, 319.

minimum-error control system.

To avoid some redundancy, the expression, rate gyro-servo, will mean rate gyro and servomotor combination throughout the remainder of the paper.

The procedure for obtaining the over-all frequency response and the method of adjusting the gains was as follows. The frequency responses of the missile and the rate gyro-servo were plotted and the product, $\frac{\delta_r}{\delta}(j\omega) = \frac{\theta_o}{\delta}(j\omega) \cdot \frac{\delta_r}{\theta_o}(j\omega)$, was taken by adding the log modulus and the phase angles on the graphs of log modulus plotted against log frequency, and phase angle against log frequency. This product was then plotted on the Nichols chart and the closed-loop frequency response, $\frac{\delta_r}{\delta_A}(j\omega)$, was obtained by reading the coordinates of the superimposed closed-loop contours. At this point, the static gain of the rate gyro-servo can be increased or decreased by merely translating the open-loop curve vertically to a higher or lower position, respectively. Then the following operation was necessary to obtain the $\frac{\theta_o}{\delta_A}(j\omega)$ frequency response:

$$\frac{\theta_o}{\delta_A}(j\omega) = \frac{\delta_r}{\delta_A}(j\omega) \cdot \frac{\theta_o}{\delta_r}(j\omega)$$

The autopilot transfer function was added to this response on the graphs of log modulus plotted against log frequency, and phase angle against log frequency to yield the over-all open-loop response, $\frac{\theta_o}{\epsilon_1}(j\omega)$.

At this point, any variation of the rate gyro-servo static gain altered the shape of the open-loop frequency-response curves, $\frac{\theta_o}{\tau_1}(j\omega)$, and a family of curves for each missile and autopilot combination was produced for several values of rate gyro-servo static gains. This family of curves was examined, and the curve whose modulus approximated the shape of the closed-loop zero-decibel contour on the Nichols chart and had a large pass band of frequencies was chosen as that which would yield nearly a minimum-error transient response for the missile with that particular autopilot; then the autopilot static gain was adjusted to position the open-loop curve so it fell somewhere along the zero-decibel contour or between the zero- and 2.3-decibel contours, depending on the shape of the curve. When this gain adjustment was made, the over-all closed-loop response, $\frac{\theta_o}{\theta_i}(j\omega)$, was obtained by reading the coordinates on the superimposed closed-loop contours. This was the final step in finding the attitude-angle response to a sinusoidal signal, $\theta_i(j\omega)$. Having found this response, the attitude-angle transient response to a square-wave input was obtained by the method of superposition. See Appendix B for examples of the log-modulus and phase-angle plots and Nichols charts.

Since it is not always possible by merely examining slightly different frequency responses to choose the one that will result in the best transient characteristics, it

was necessary to obtain and examine the transient responses for several adjustments of K_r and K_A by the method described in the previous paragraph, and the combination of K_A and K_r which yielded the best transient characteristics was selected. This method of adjusting the system's gains did not necessarily give a minimum-error transient response, but it was believed to have given one which was nearly minimum. The gains were thus adjusted for each autopilot at $M = 1.6$ and an altitude of 4,000 feet.

Holding these gains fixed, the attitude-angle transient responses for other Mach numbers and altitudes were obtained by the method previously mentioned after making the required changes in the coefficients of the missile's transfer function.

The procedure for obtaining the control-surface-deflection and normal-acceleration transient responses to a step command signal was the same except for the previously mentioned changes in the block diagram described in Chapter II.

Method of obtaining the transient responses. The transient responses were obtained by the use of an electromechanical Fourier synthesizer at the Langley Laboratory. This machine adds a finite number of terms of a Fourier series.[3] Since the frequency response of the system

[3] Seamans, Bromberg, and Payne, loc. cit.

including the missile, rate gyro-servo, and the autopilot was available, the system's response to a square-wave input was determined by the method of superposition. The output produced was

$$\frac{2}{\pi} \sum_{n=1,3,5\ldots23} \left[\frac{\text{Amplitude ratio}_{n\omega_1}}{n} \right] \sin \left[n\omega_1 t + (\text{Phase angle})_{n\omega_1} \right]$$

One requirement was that it was necessary to have the period of the fundamental frequency, ω_1, large enough so that all of the transient motion had essentially died out by the end of each half cycle. Twelve odd harmonics usually gave a good approximation for the response of the system to a square-wave input. The rate-damped missile and autopilot were equivalent to an electrical low-pass filter so that any high-frequency harmonics were greatly attenuated relative to the fundamental and thereby contributed little to the transient response.

CHAPTER IV

RESULTS AND DISCUSSION

The analysis was conducted to determine the effects of the natural frequency of autopilots on the performance characteristics of an attitude control system. Nearly minimum-error transient responses of the rate-damped missile and autopilot combination were obtained for M = 1.6 and an altitude of 4,000 feet with suitable adjustments of the rate gyro-servo and autopilot static gains. These resulting gain constants with the corresponding autopilot natural frequencies are presented in Table II. With these same gains, attitude-angle transient responses for flight conditions, M = 1.2 and M = 2.0 at an altitude of 4,000 feet and M = 1.6 at an altitude of 30,000 feet, were obtained to determine the effects on the system due to changes in flight conditions. Also, control-surface-deflection transient responses were found for flight conditions, M = 1.2, M = 1.6, and M = 2.0 at 4,000 feet, and all flight conditions considered for the missile with an autopilot having a natural frequency of 50 radians per second. Normal-acceleration transient responses were obtained for the autopilot natural frequency of 50 radians per second for all flight conditions considered and for all other autopilots at M = 2.0 and 4,000 feet.

In studying the results herein, there are three

TABLE II

AUTOPILOT AND RATE-GYRO-SERVO STATIC GAINS TABULATED AGAINST AUTOPILOT NATURAL FREQUENCY

[Adjusted for M = 1.6 and altitude of 4,000 feet]

ω_n	K_r	K_A
140	0.08	2.32
70	.13	2.43
50	.16	2.82
30	.10	1.26

salient transient characteristics appearing in this discussion that need to be defined: amplitude of the initial overshoot, rise time, and response time. The amplitude of the initial overshoot is the magnitude of the first peak above and measured from the steady-state value. The rise time is the time for the output, $\theta_o(t)$, to initially reach the steady-state value. The response time is the time required for the output to reach and remain within ± 5 percent of the steady-state or final value. These salient attitude-angle transient characteristics are illustrated in Figure 7. Since the output of most physical systems can at best only follow the input with some small dynamic error, the best approximation of a desired transient response is the one that has a small amplitude for the initial overshoot, a short rise time, and a short response time. Desirable transient-response characteristics are those that reduce the transient dynamic error; however consideration of the structural and the control-surface-deflection rate limitations may put some restrictions on these transient characteristics. Also, a missile and autopilot combination may have transient characteristics that are desirable for one flight condition, but changes in Mach number or altitude may cause a radical change in the amplitude of the initial overshoot, response time, and rise time. Another system may have transient characteristics that yield a slow response or one with appreciable transient

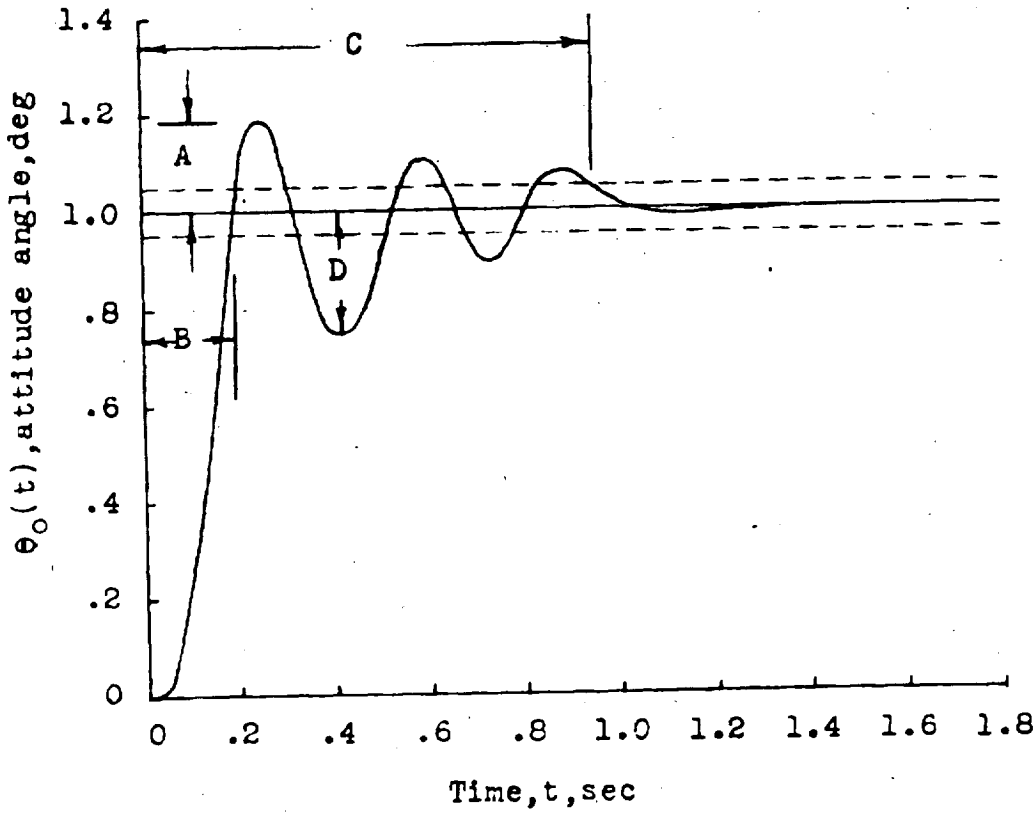

A - Amplitude of the initial overshoot

B - Rise time

C - Response time

D - Transient error

Figure 7.- Representative attitude-angle transient response illustrating transient characteristics: amplitude of the initial overshoot, response time, rise time, and transient error

error, and yet, changes in flight conditions may not have much effect on these transient characteristics. It may become necessary, depending on the application, to sacrifice desirable transient characteristics for poorer transient characteristics that are more consistent over a Mach number and altitude range. The particular application of the control system will dictate what considerations are necessary for effective control.

A physical system may exhibit non-linear behavior caused by some limitation on the control-surface deflection either due to stops built into the control system, finite length of the servomotor stroke, or limit on the aerodynamic control effectiveness. For example, in order to produce the required attitude-angle transient response, the inputs to the servomotors may call for a large oscillatory control-surface angular displacements through the combined outputs of the rate gyro-servo and autopilot causing the servomotors to limit at a maximum angular deflection and to remain there until the signals to the servomotors call for a reduction in the control-surface deflection from this maximum value.

The linear analysis for the control system may also call for a rate of servomotor displacement that is beyond the physical limit of a particular valve and servomotor combination. This power limitation, which, for example, might be due to some restriction in the time rate of volume flow for

a hydraulic fluid under a given pressure, was not considered in the analysis. The transfer function for the autopilot was based upon the servomotor ouput velocity, $\dot{x}$, being proportional to the transfer valve displacement, y. This linearization of the valve flow characteristics and the assumption of incompressible flow yielded the second-order characteristic equation of the autopilot. See Appendix A.

Precautions should be taken to prevent such non-linear behavior in a control system. If, however, such behavior does exist, consideration should be given to determine to what extent the linear method of analysis is valid.

Attitude-angle transient responses. Attitude-angle transient responses are presented in Figures 8 through 11. The transient characteristics are summarized in Figures 12 and 13.

Figure 12 shows that, in general, increasing the natural frequency of the autopilot for all Mach numbers and altitudes considered causes the rise time and the response time to decrease. The initial overshoot did not have any significant trend so it was neglected.

Figure 13 also shows that the greatest improvement in the transient characteristics occurs for the system with an autopilot natural frequency between 30 and 70 radians per second. For the system with an autopilot natural frequency greater than 70 radians per second, the improvement is not so

$$\text{Autopilot} = \frac{K_A \omega_n^2}{s^2 + 2\zeta\omega_n s + \omega_n^2} \qquad \zeta = .5 \quad \omega_n = 30$$

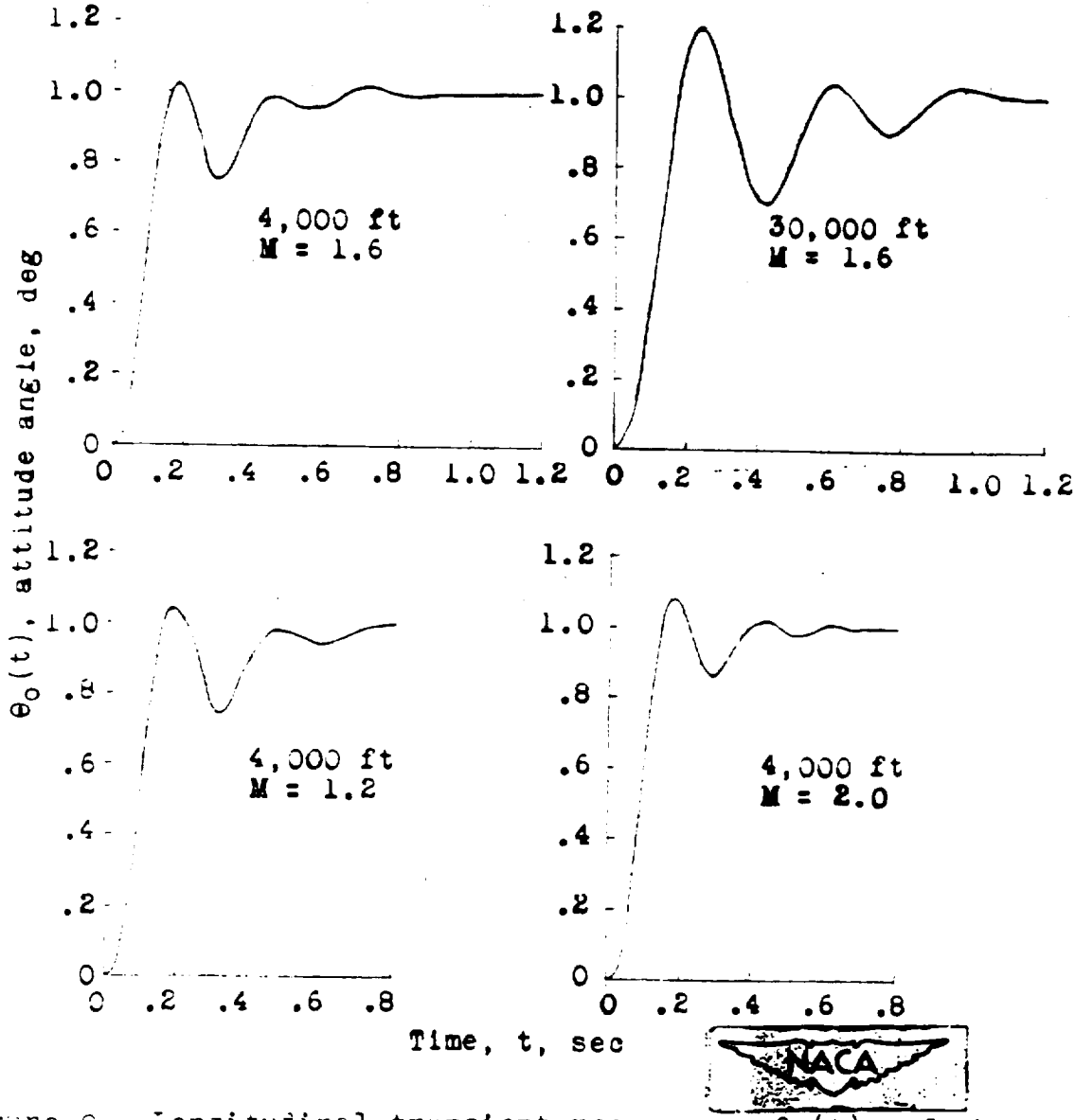

Figure 8.- Longitudinal transient responses, $\theta_o(t)$, of the control system to a unit step input signal calling for a change in attitude of 1°. $K_r = 0.10$; $K_A = 1.26$.

$$\text{Autopilot} = \frac{K_A \omega_n^2}{s^2 + 2\zeta\omega_n s + \omega_n^2} \qquad \zeta = .5 \quad \omega_n = 50$$

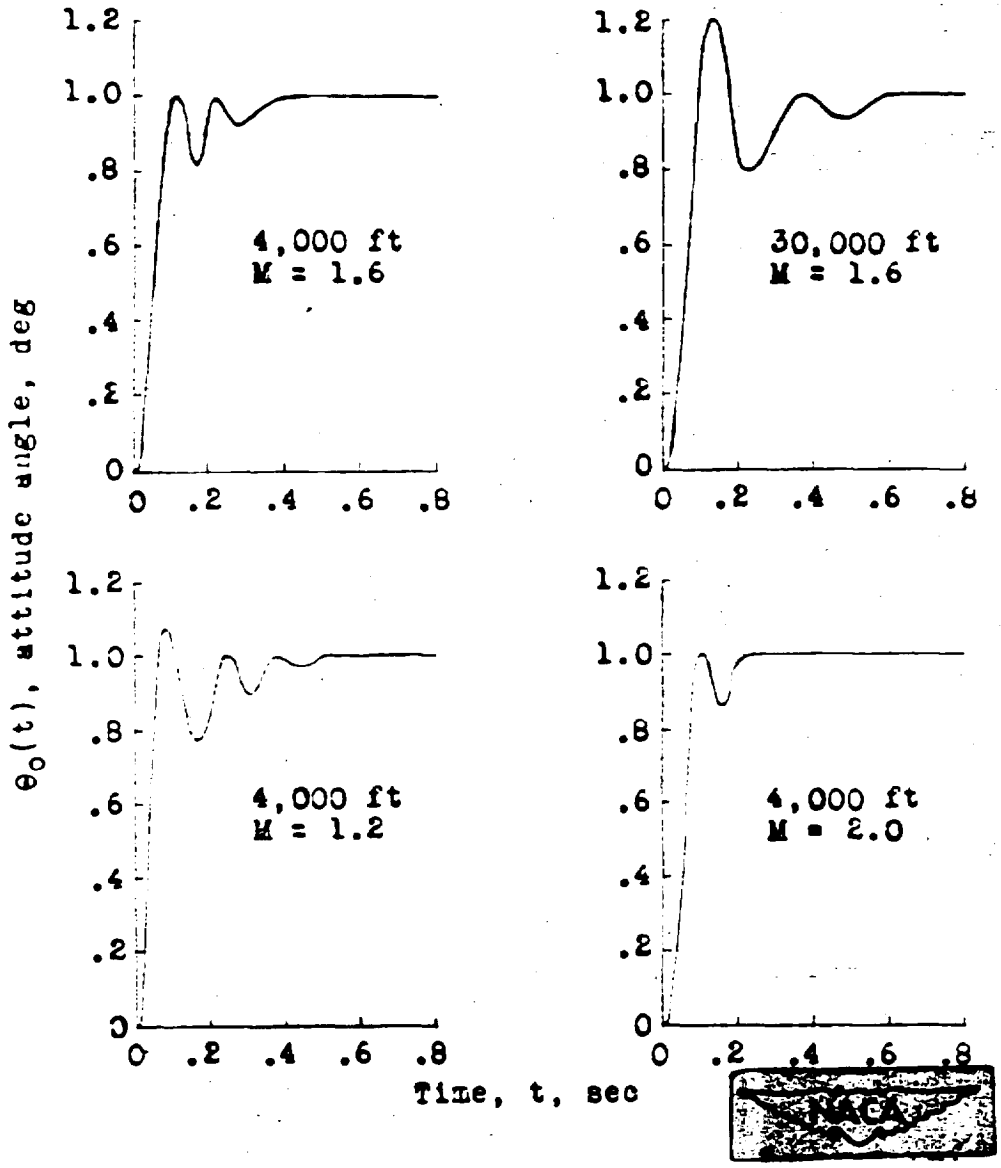

Figure 9.- Longitudinal transient responses, $\theta_o(t)$, of the control system to a unit step input signal calling for a change in attitude of 1°. $K_r = 0.16$; $K_A = 2.82$.

$$\text{Autopilot} = \frac{K_A \omega_n^2}{s^2 + 2\zeta\omega_n s + \omega_n^2} \qquad \zeta = .5 \quad \omega_n = 70$$

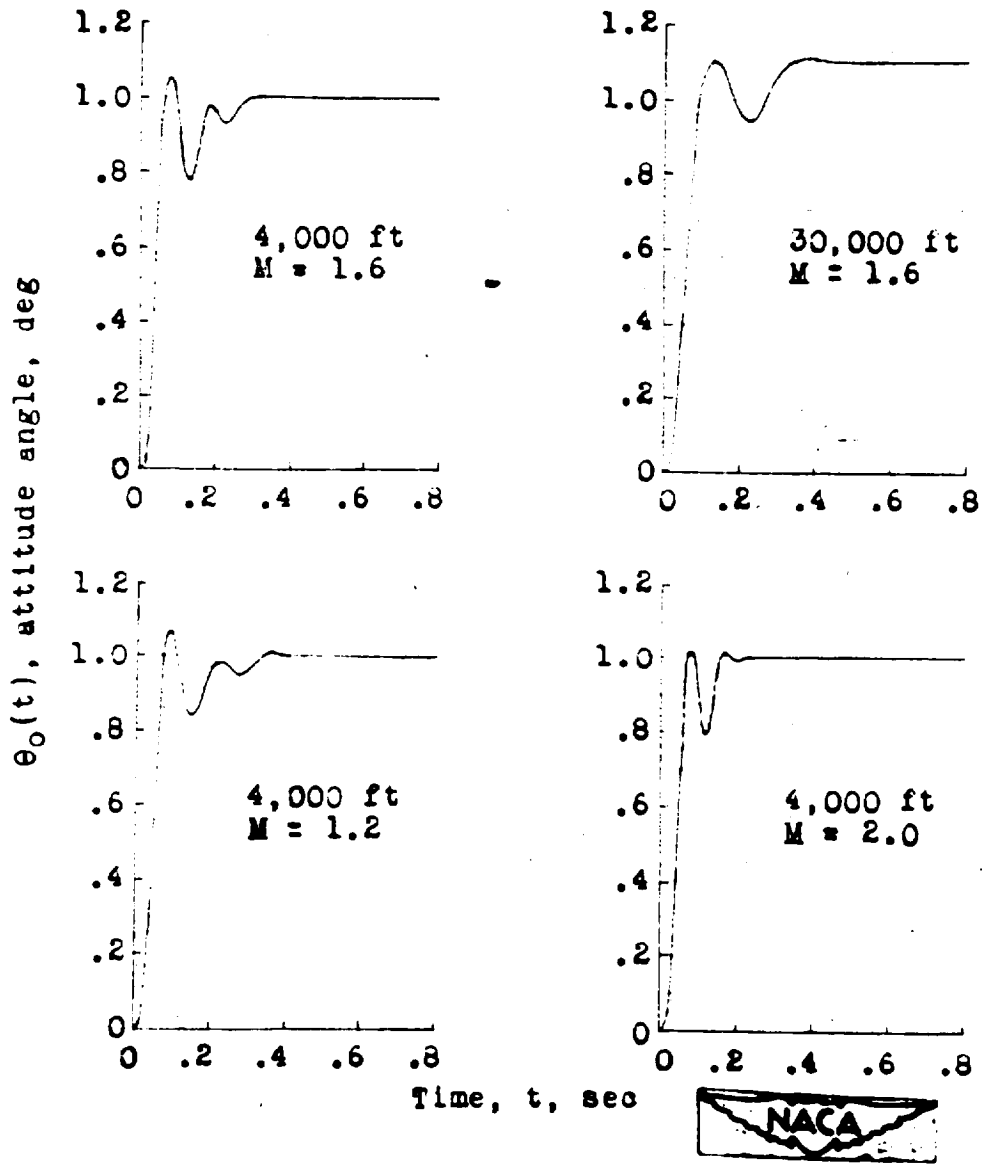

Figure 10.- Longitudinal transient responses, $\theta_o(t)$, of the control system to a unit step input signal calling for a change in attitude of 1°. $K_r = 0.13$; $K_A = 2.43$.

$$\text{Autopilot} = \frac{K_A \omega_n^2}{s^2 + 2\zeta\omega_n s + \omega_n^2} \qquad \zeta = .5, \quad \omega_n = 140$$

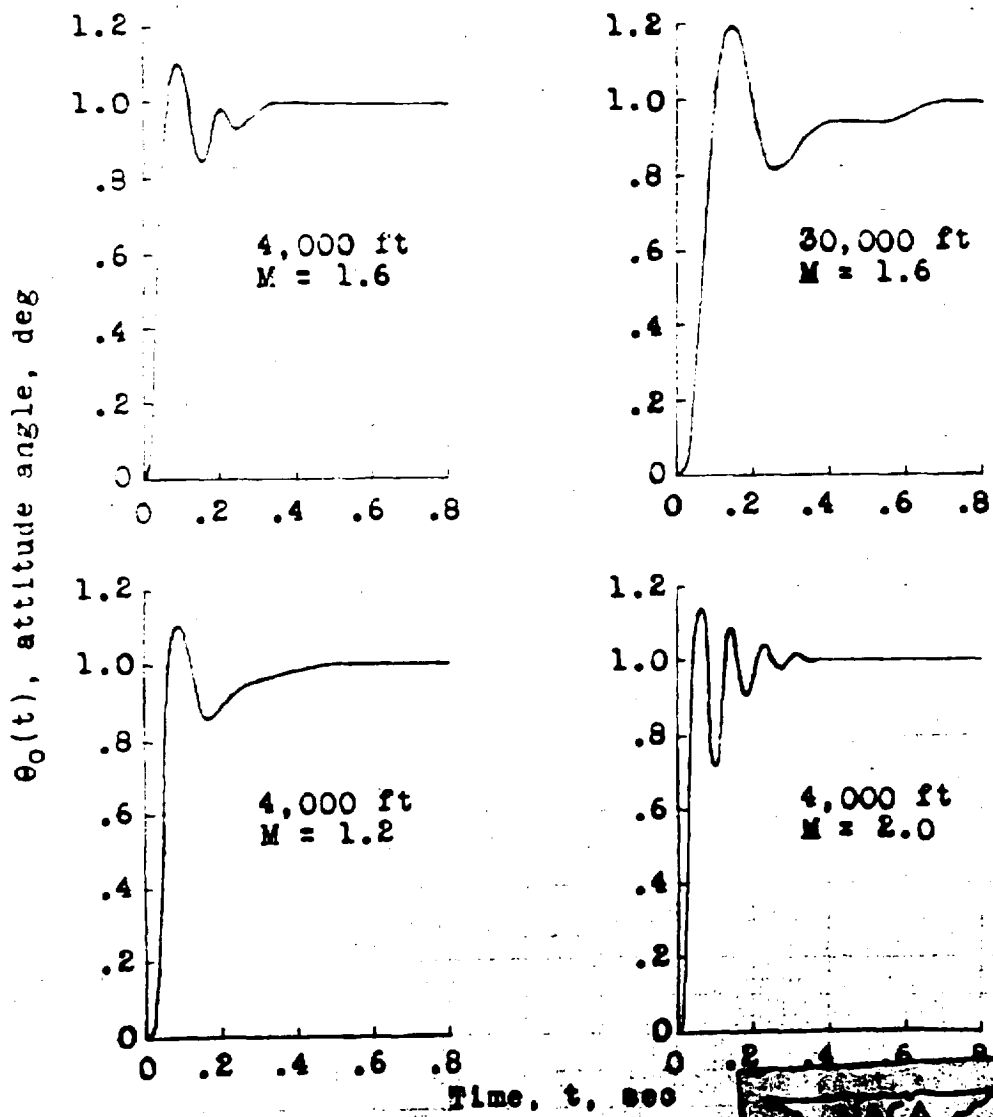

Figure 11.- Longitudinal transient responses, $\theta_o(t)$, of the control system to a unit step input signal calling for a change in attitude of 1°. $K_r = 0.08$; $K_A = 2.32$.

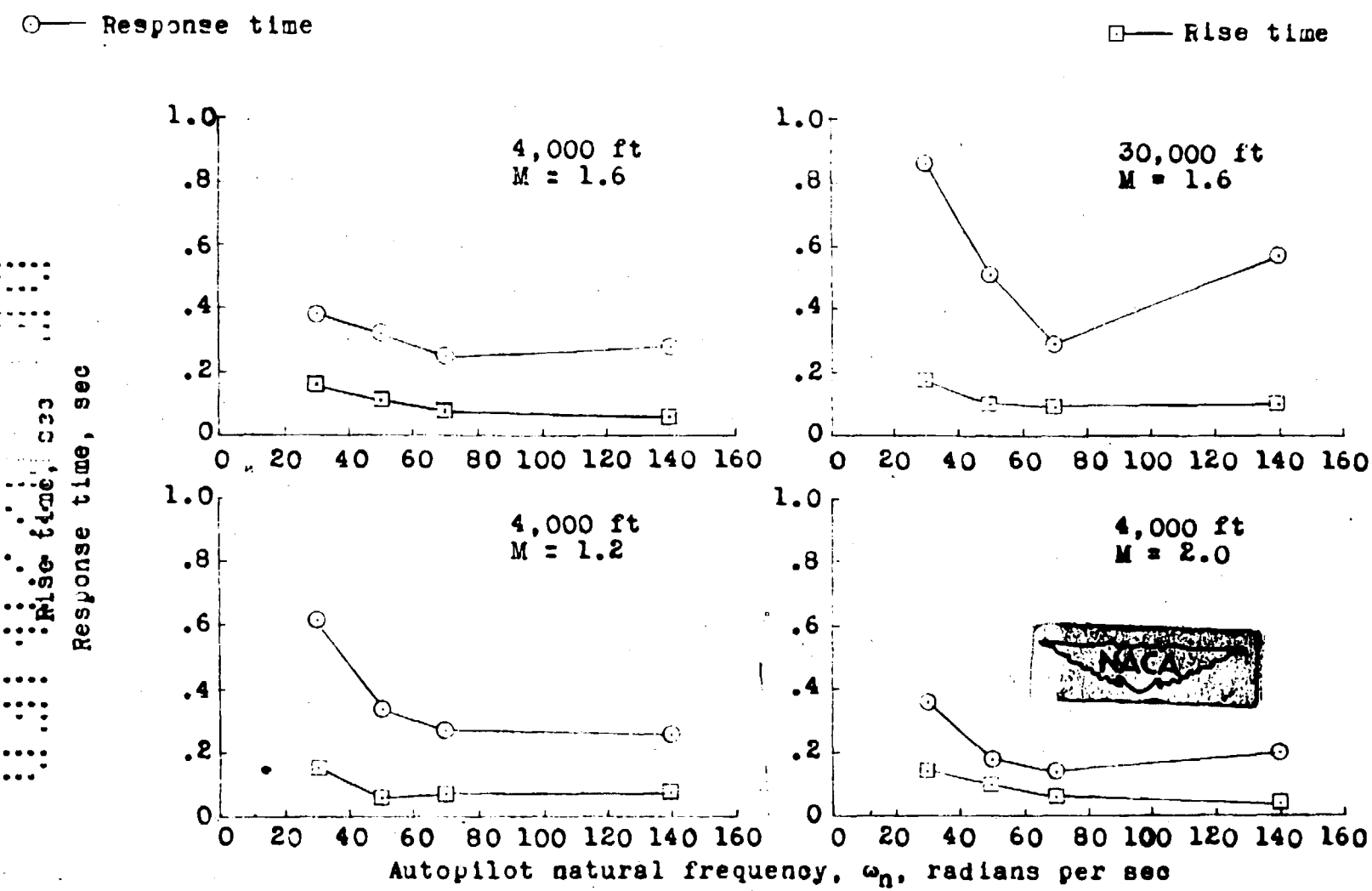

Figure 12.- Attitude-angle transient characteristics, response time and rise time, plotted against autopilot natural frequency. ζ of autopilot, 0.5.

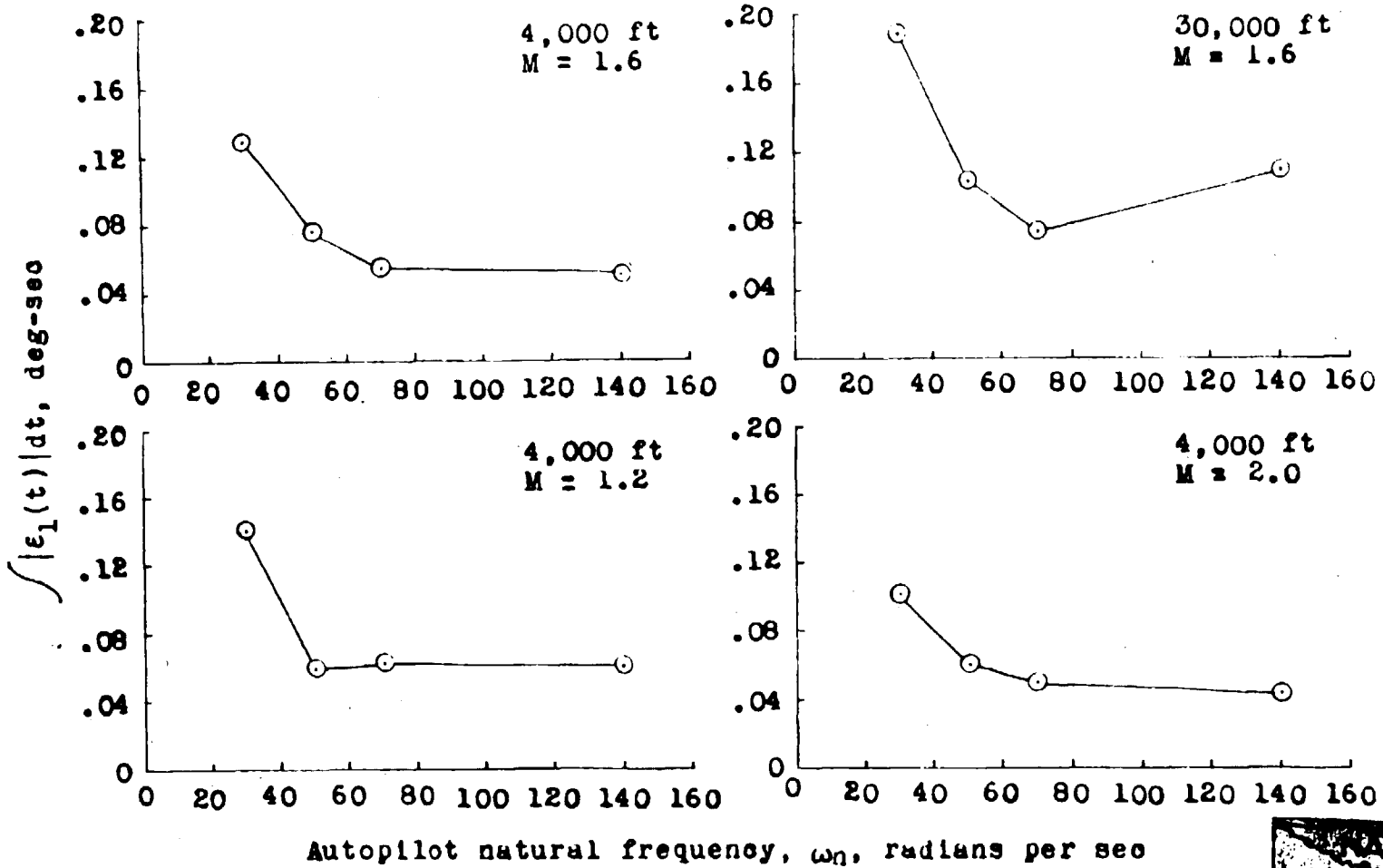

Figure 13.- Plot of $\int|\epsilon_1(t)|dt$ for the rate-damped missile and autopilot combination against autopilot natural frequency in response to a step θ_1. ζ of autopilot, 0.5.

pronounced; however at these frequencies, the cost in the design and construction of such autopilots begins to increase appreciably. For an economic reason, the possible added improvement as a result of using an autopilot natural frequency greater than 70 will be outweighed by the increased cost.

The total transient error, or $\int|\epsilon_1(t)|dt$ was computed by integrating with a planimeter over the attitude-angle transient response from zero time to the time required for the output to reach and remain within 5 percent of the steady-state value. This total transient error is a method of evaluating the combined effects of the transient characteristics and is indicative of how well the output follows the input signal; the magnitude of this error should be held at a minimum for accurate control.

Since the analysis did not include an attempt to minimize any one of the transient characteristics such as the rise time, response time, or the initial overshoot, there may be some application where one, two, or all three of these characteristics must be held below some previously determined minimum. The minimum-error criteria employed in the analysis may not necessarily minimize any one of these salient characteristics unless the criteria is modified by weighting the error signal, $\epsilon_1(t)$, with some function of time, $f(t)$, yielding $\int|\epsilon_1(t)|f(t)dt$ that should be held at a minimum.

This function of time may be chosen arbitrarily to favor a transient with a short rise time, a short response time, or a small overshoot.

Further, the minimum-error criteria employed in the analysis must be used with caution whenever there is noise present in the command signal. A control system having a small value of $\int |\varepsilon_1(t)| dt$ is usually associated with a control system having a relatively large bandwidth. Figure 14 is included to illustrate the type of pass band and the magnitude of the bandwidth of the attitude control system. When a random disturbance or noise is present in the command signal, there may be unwanted motion at the output of the control system, and increasing the bandwidth will usually increase the magnitude of this unwanted motion; therefore, to reduce the effects of noise at the output, the bandwidth can be reduced with some loss in control accuracy. When a random signal is present over the entire pass band, there arises the very complex problem of determining the type of control-system frequency response that will keep the error due to noise at a minimum and the error between the desired input and output at a minimum. Obviously, some sacrifice must be made in control accuracy to reduce the effects of noise at the output. There have been some recent advancements[1] in the methods of determining the type of frequency

[1] A. Tustin, Automatic and Manual Control (New York: Academic Press Inc., 1952).

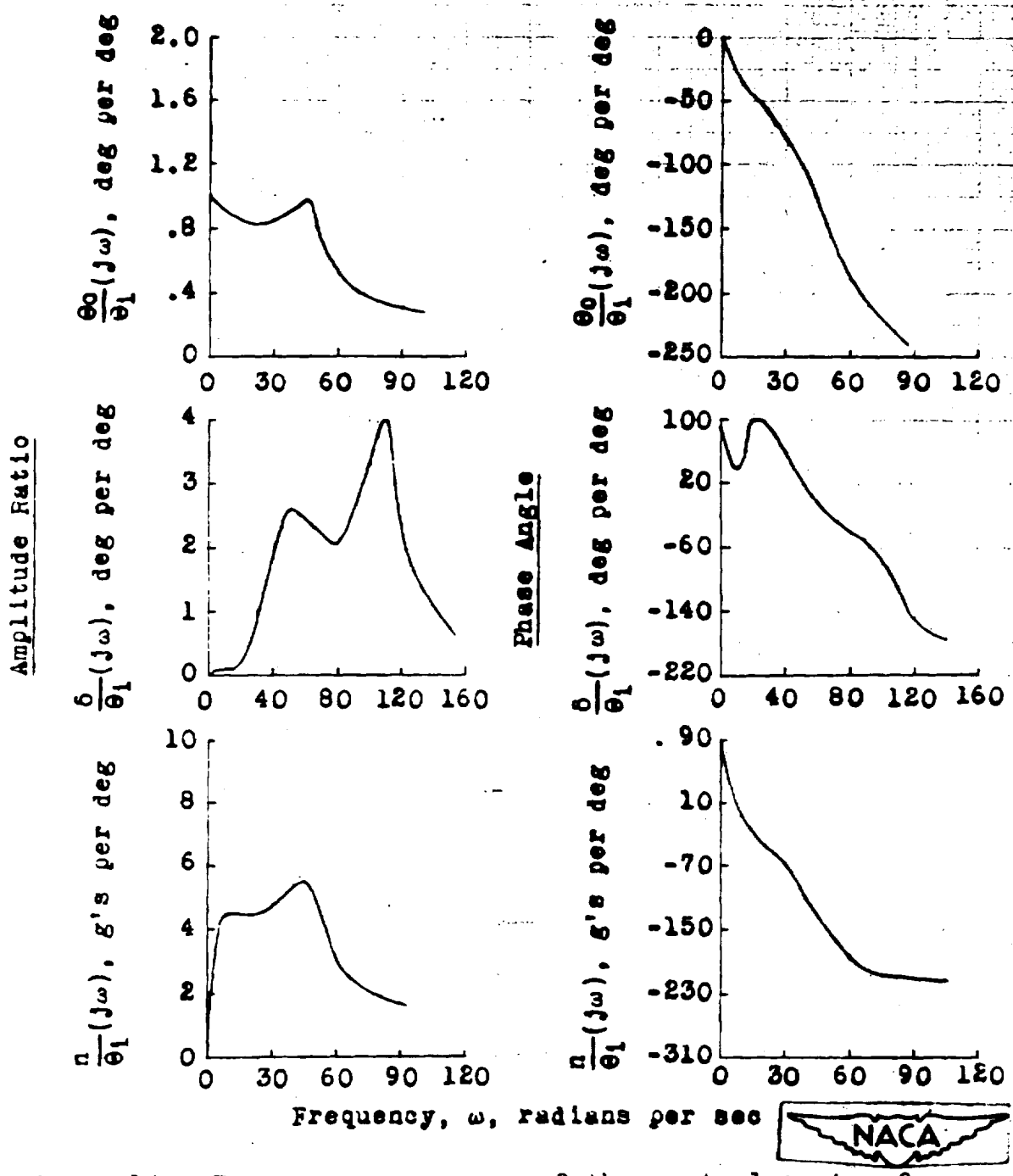

Figure 14.- Frequency responses of the control system for an autopilot natural frequency of 50 radians per sec. $K_r = 0.16$; $K_A = 2.82$; $M = 2.0$; altitude = 4,000 ft.

responses necessary for control systems with random disturbances in the input signal largely as a result of work done by Wiener.[2]

Control-surface-deflection and normal-acceleration transient responses. In order to present a more complete analysis of the rate-damped missile and autopilot combination, control-surface-deflection and normal-acceleration transient responses to a unit step input signal, $\theta_i(t)$, are presented in Figures 15 through 20. Since there are physical limitations on structural loads, amplitude of the control-surface angular deflections, and time rates of change of the control-surface deflections, these transients are useful in determining what maximum values to expect for any step input signal. Also, the δ transient responses indicate what total accumulator energy and what peak accumulator power is required in response to a step input, $\theta_i(t)$.

Control-surface-deflection transient responses were obtained for the missile and autopilot combination with the autopilot natural frequencies of 30, 50, 70, and 140 radians per second and for an altitude of 4,000 feet at all Mach numbers considered. A response was also obtained for an autopilot natural frequency of 50 radians per second at

[2] N. Wiener, Interpolation, Extrapolation, and Smoothing of Stationary Time Series (New York: John Wiley and Sons, 1949).

$$\text{Autopilot} = \frac{K_A \omega_n^2}{s^2 + 2\zeta\omega_n s + \omega_n^2} \qquad \zeta = .5 \quad \omega_n = 30$$

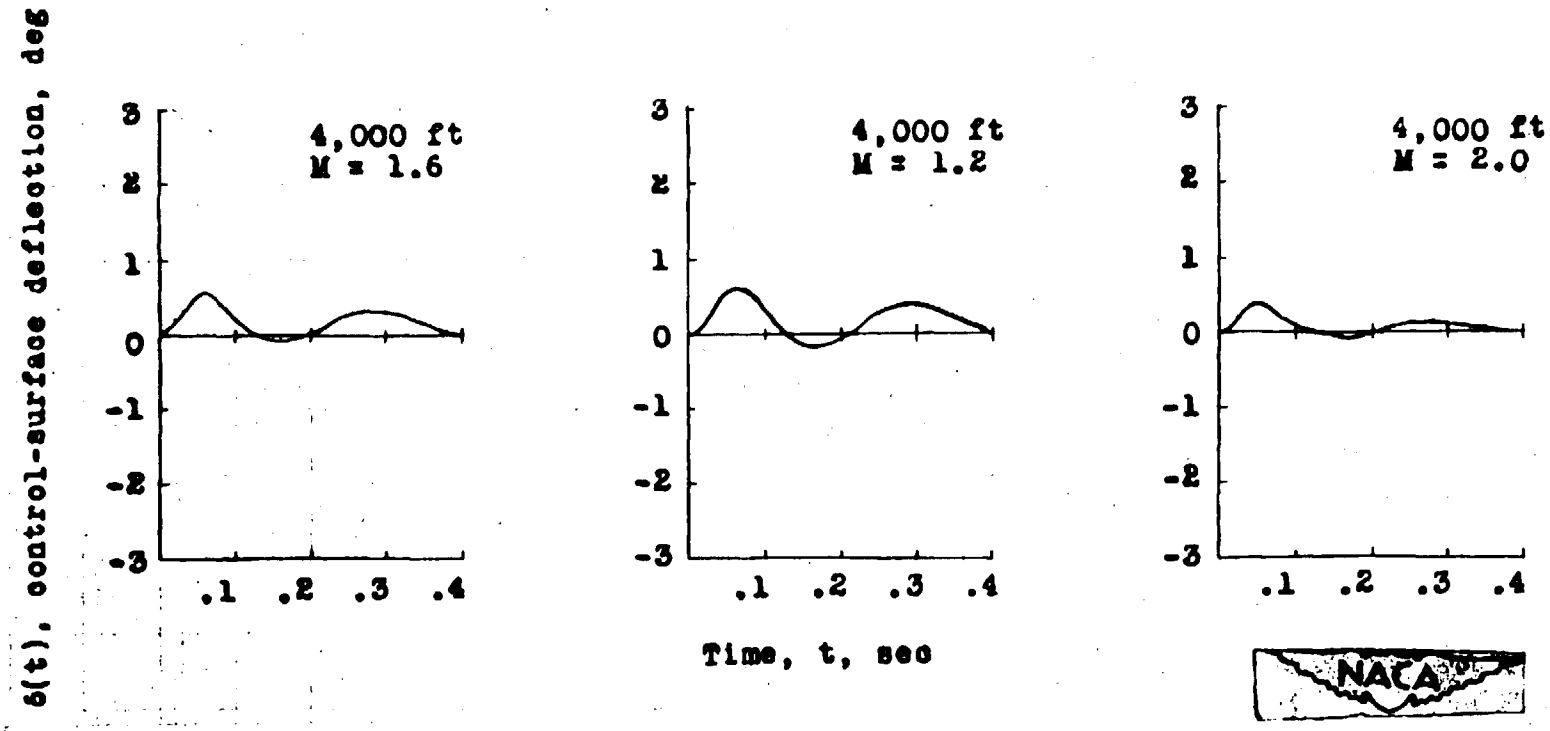

Figure 15.- Longitudinal transient response, δ(t), of the control system to a unit step input signal calling for a change in attitude of 1°. $K_r = 0.10$; $K_A = 1.26$.

$$\text{Autopilot} = \frac{K_A \omega_n^2}{s^2 + 2\zeta\omega_n s + \omega_n^2} \qquad \zeta = .5 \quad \omega_n = 50$$

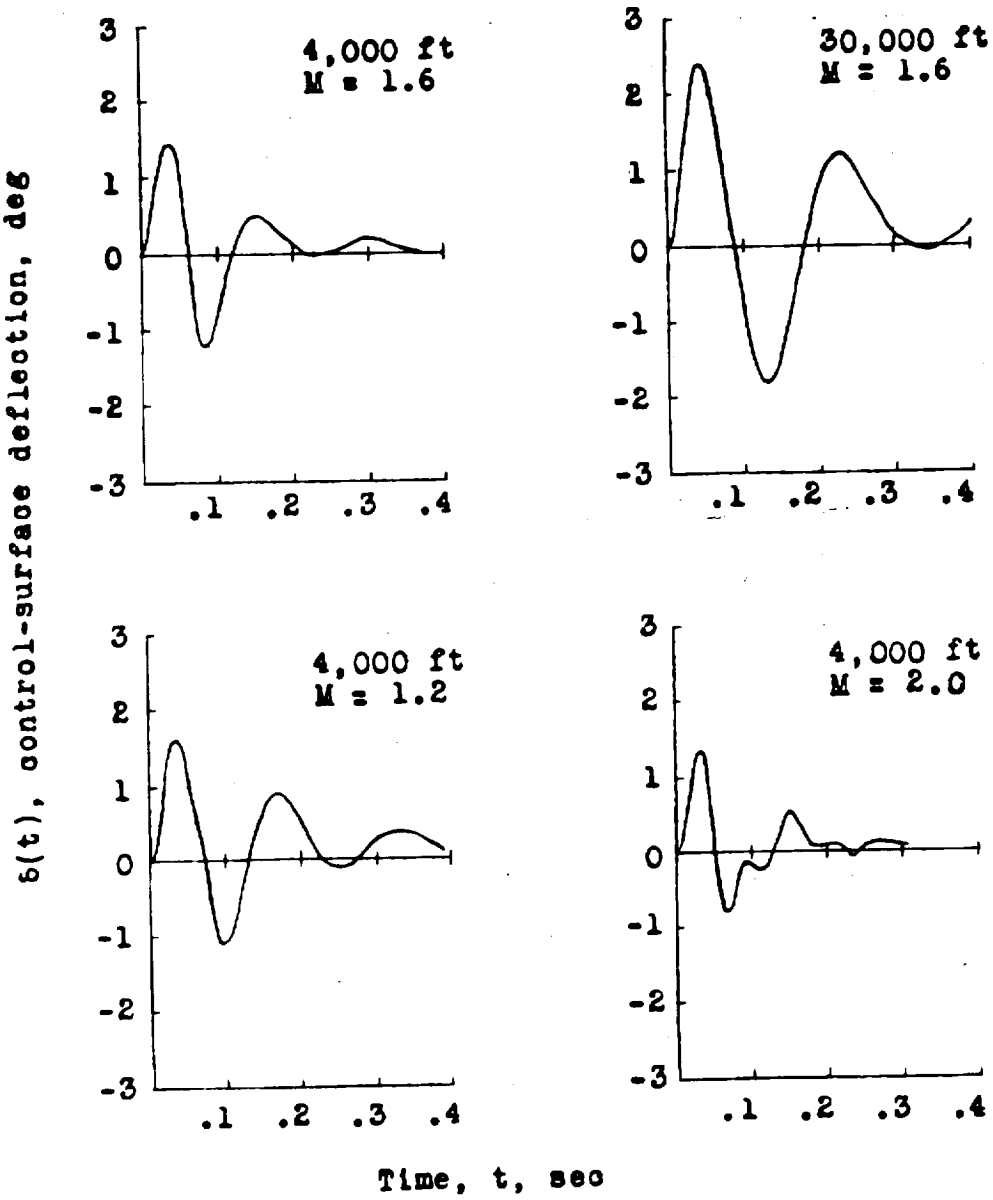

Figure 16.- Longitudinal transient response, δ(t), of the control system to a unit step input signal calling for a change in attitude of 1°. $K_r = 0.16$; $K_A = 2.82$.

CONFIDENTIAL
SECURITY INFORMATION

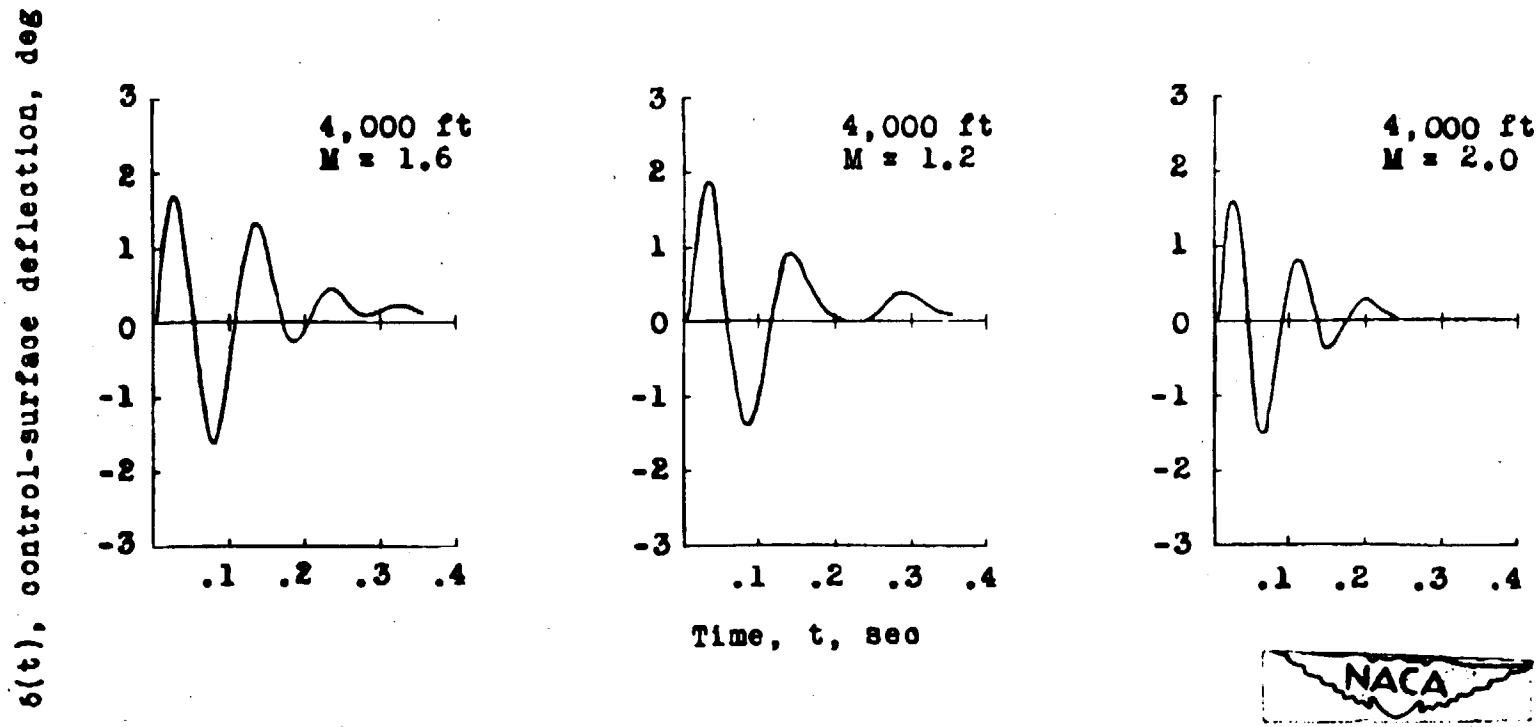

Figure 17.- Longitudinal transient response, δ(t), of the control system to a unit step input signal calling for a change in attitude of 1°. $K_r = 0.13$; $K_A = 2.43$.

CONFIDENTIAL

$$\text{Autopilot} = \frac{K_A \omega_n^2}{s^2 + 2\zeta\omega_n s + \omega_n^2} \qquad \zeta = .5 \quad \omega_n = 140$$

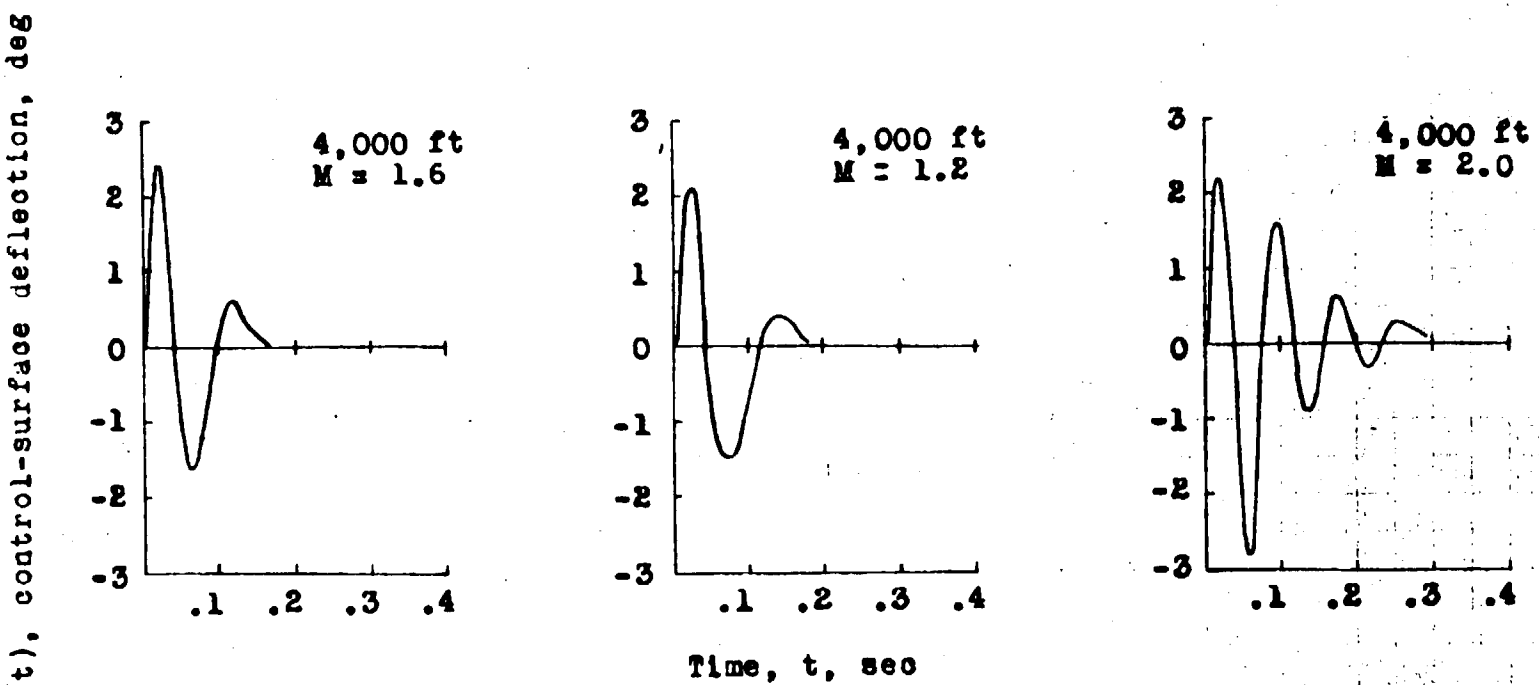

[redacted]

Figure 18.- Longitudinal transient response, δ(t), of the control system to a unit step input signal calling for a change in attitude of 1°. $K_r = 0.08$; $K_A = 2.32$.

$$\text{Autopilot} = \frac{K_A \omega_n^2}{s^2 + 2\zeta\omega_n s + \omega_n^2} \qquad \zeta = .5 \quad \omega_n = 50$$

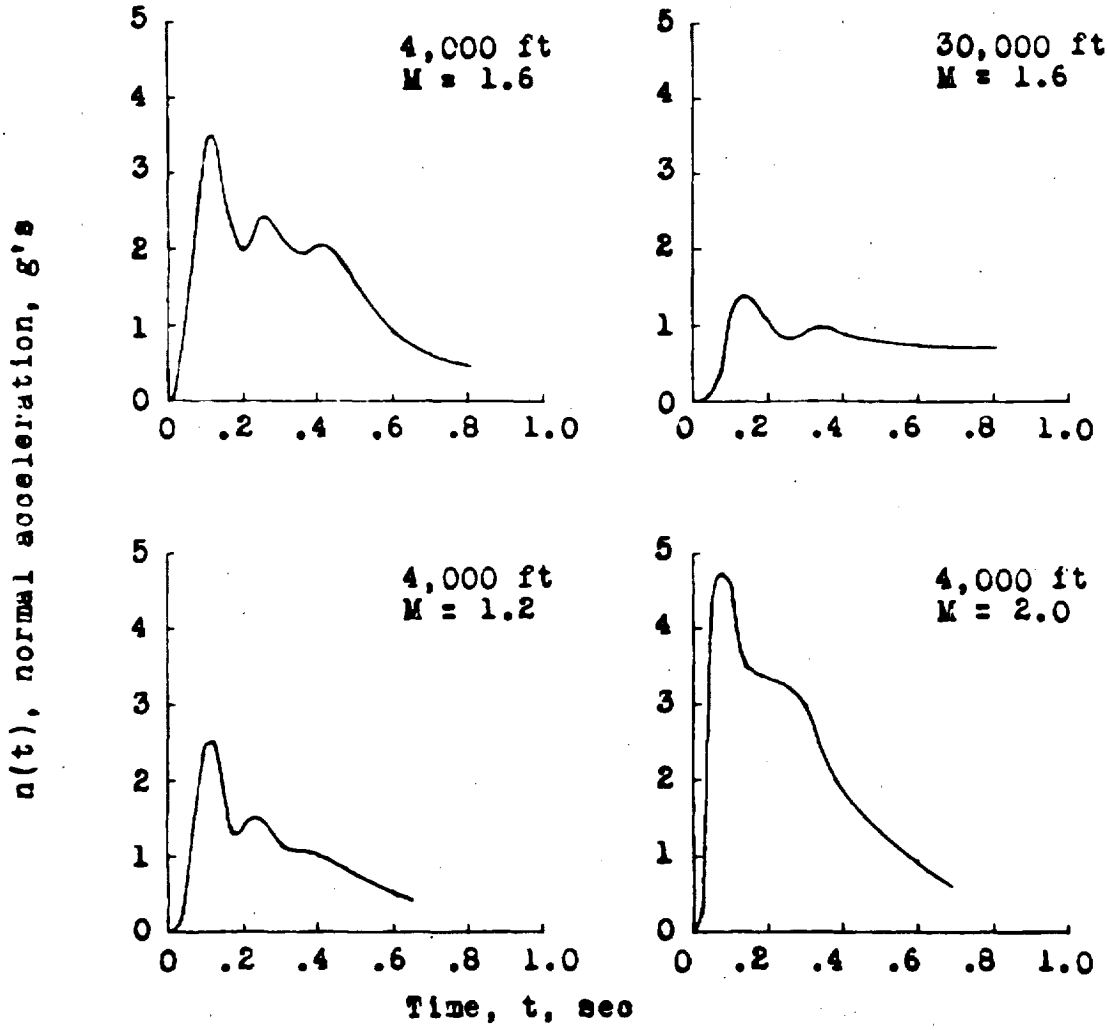

Figure 19.- Longitudinal transient response for normal acceleration, n(t), of the control system to a unit step input signal calling for a change in attitude of 1°. $K_r = 0.16$; $K_A = 2.82$.

$$\text{Autopilot} = \frac{K_A \omega_n^2}{s^2 + 2\zeta\omega_n s + \omega_n^2}$$

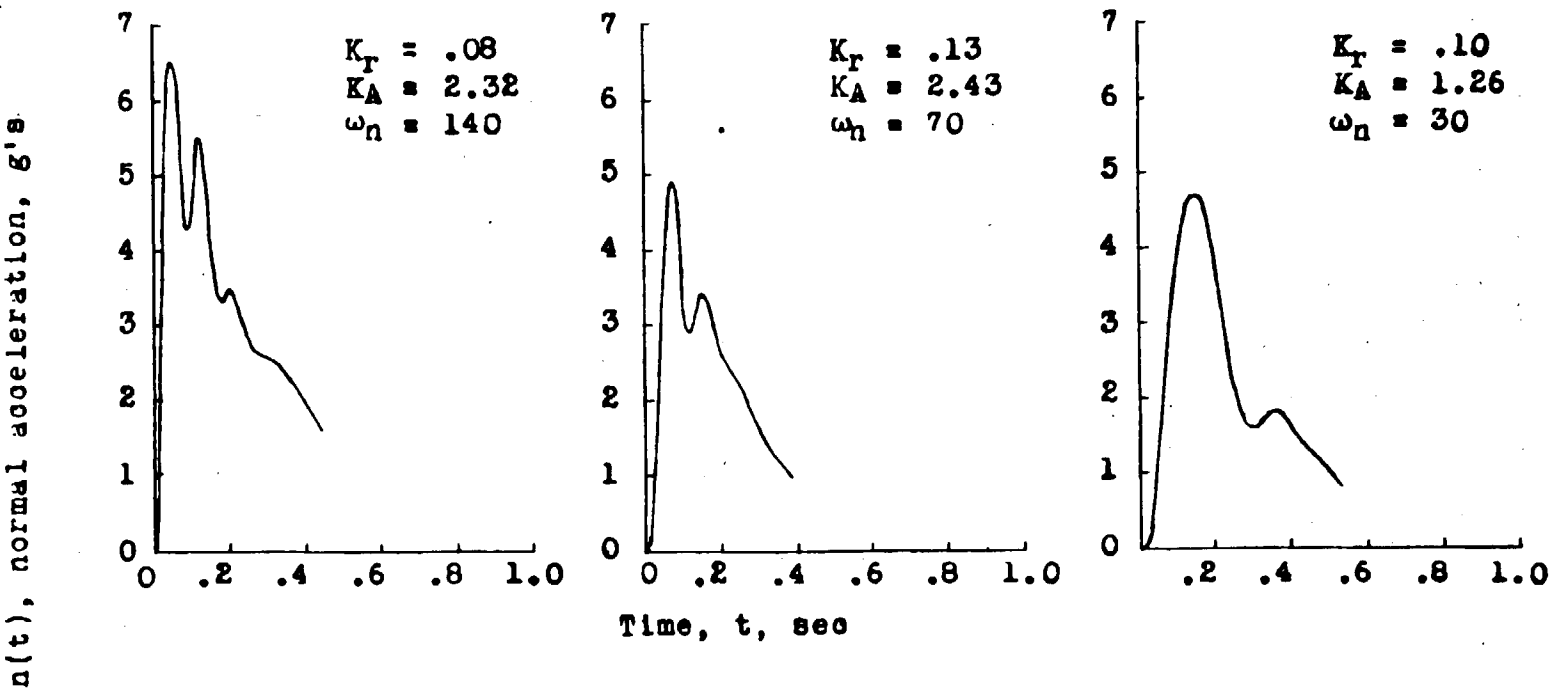

Figure 20.- Longitudinal transient responses for normal acceleration, n(t), of the control system to a unit step input signal calling for a change in attitude of 1°. M = 2.0; altitude, 4,000 feet; ζ of autopilot, 0.5.

$M = 1.6$ and an altitude of 30,000 feet.

Reviewing the δ transients presented, some general conclusions are reached. For the missile and all autopilots considered, the amplitude of the maximum control-surface deflection, in general, decreases with an increase in Mach number for an altitude of 4,000 feet. For flight conditions at 4,000 feet and all Mach numbers considered, increasing the ω_n of the autopilot increases the amplitude of the maximum overshoot. The maximum control-surface deflection for a step input signal, $\theta_i(t)$, increases with an increase in altitude for the autopilot with an $\omega_n = 50$ at $M = 1.6$.

Figure 21 presents the total δ travel, in response to a step input signal, computed from the δ transient responses. This total δ travel, or $\int \left|\frac{d\delta}{dt}\right| dt$, was obtained by manually adding the total angular displacements of the δ transient responses. The accumulator supplies the hydraulic fluid to the transfer valve and servomotor combination. Because of the assumption of incompressible flow, the volume of fluid supplied to the servomotor is proportional to the servomotor displacement which is, in turn, proportional to the control-surface angular displacement. A further assumption is that the fluid in the accumulator is under constant pressure. Reference to the accumulator energy supplied to the servomotors in this paper is the product of the constant accumulator pressure and the volume of hydraulic

$$\text{Autopilot} = \frac{K_A \omega_n^2}{s^2 + 2\zeta\omega_n s + \omega_n^2}$$

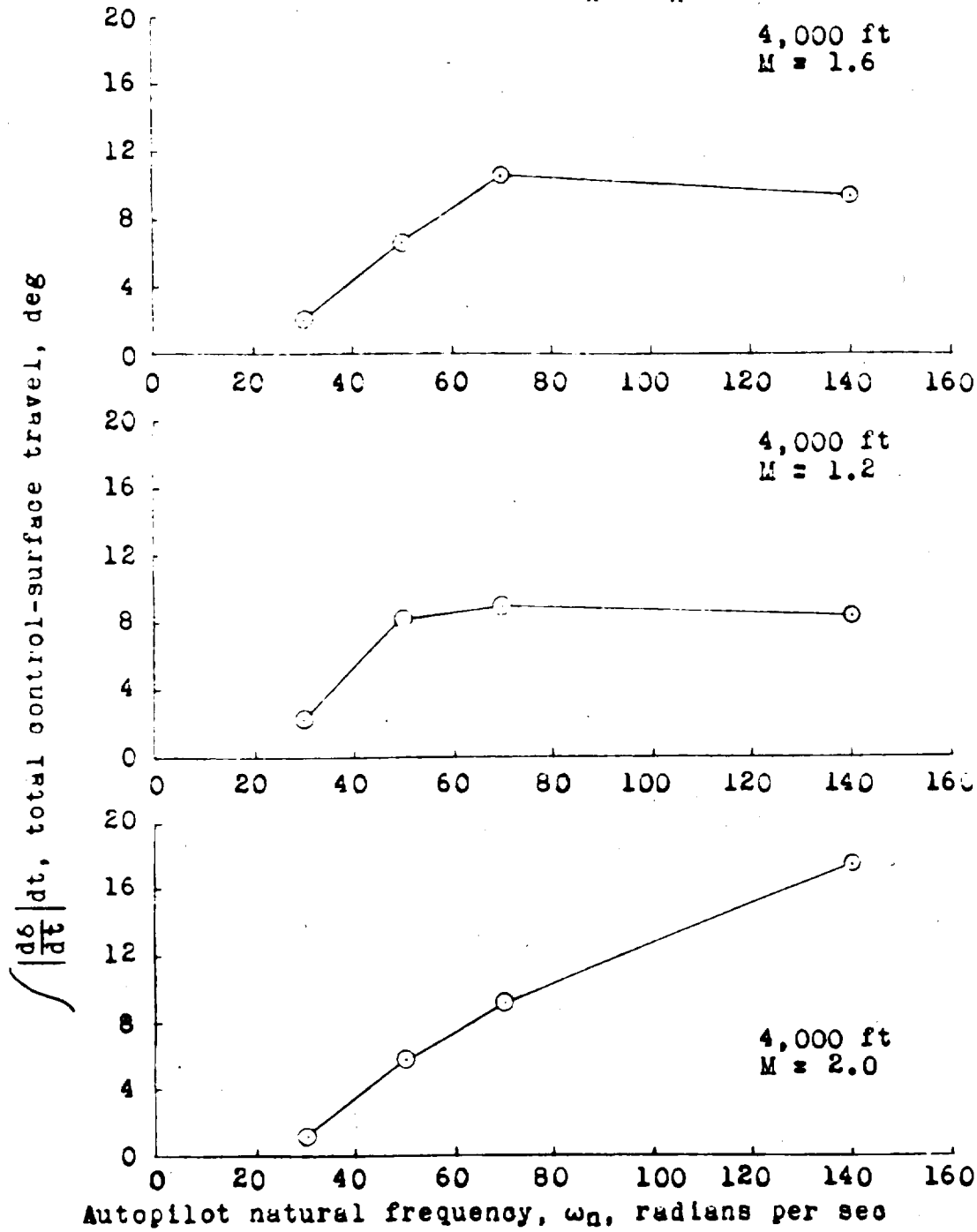

Figure 21.- Plot of total δ travel against autopilot natural frequency in response to a unit step input signal. ζ of autopilot, 0.5.

fluid supplied to the servomotors. The accumulator peak power supplied is the maximum rate at which this energy is exhausted at any instant by the servomotors in response to a step input signal.

Figure 21 illustrates that more accumulator stored energy is required for the high natural frequency autopilots than for the low frequency. In general, the accumulator energy supplied does not increase appreciably above the natural frequency of 70 radians per second.

Figures 15 through 18 illustrate that the peak power required of the accumulator is higher for the system with the higher natural frequency. To supply this peak power, the restrictions to the flow of fluid should be kept at a minimum by making the cross-sectional areas of the valve and servomotor ports along with the connecting tubing large. Since this requires that the accumulator and the associated gear be large physically, the space and weight limitations make it a requirement to keep the natural frequency near the lowest value that yields satisfactory control accuracy.

Normal-acceleration transient responses were obtained for the system having an autopilot natural frequency of 50 radians per second for all Mach numbers and altitudes considered and for the system with the four autopilots considered at the highest Mach number. The highest Mach number was chosen since this flight condition usually yields

the highest value of ζ for a given altitude, and would set the limit on the maximum amplitude of the input step signal so that the missile will not be stressed near its structural limit while responding to commands. The normal-acceleration transient responses shown for $M = 2.0$ illustrate that as ω_n increases, the maximum normal acceleration increases. For $\omega_n = 50$ and $M = 1.6$, increasing the altitude decreases the maximum normal acceleration per degree of input, $\theta_1(t)$. Finally, for the autopilot $\omega_n = 50$ at 4,000 feet, increasing the Mach number increases the maximum overshoot for the $n(t)$ transient response. Figure 22 illustrates that the structural limit is approached rapidly as the autopilot natural frequency reaches 140 radians per second.

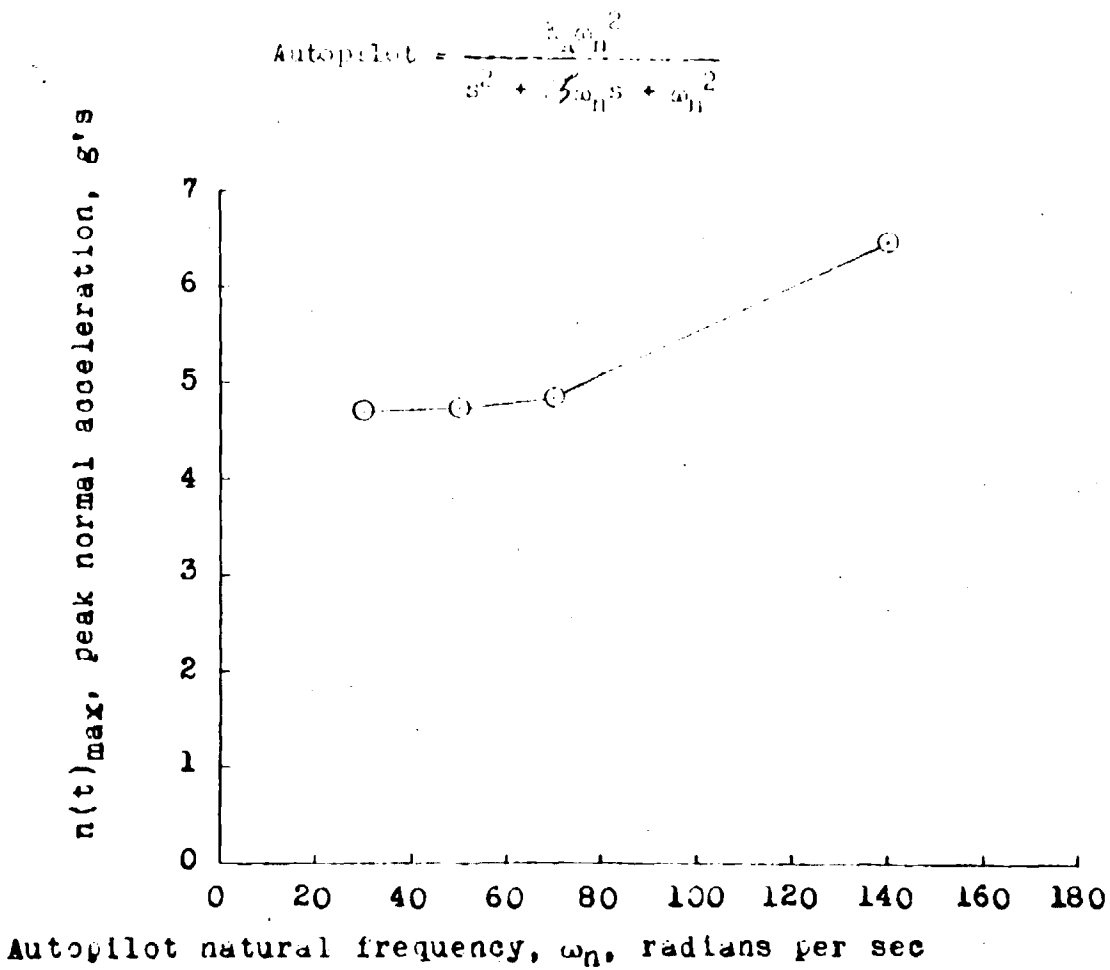

Figure 22.- Plot of $n(t)_{max}$ against autopilot natural frequency in response to a step input signal. M = 2.0; altitude, 4,000 feet.

CHAPTER V

CONCLUSIONS

As a result of the theoretical investigation of the influence of an autopilot natural frequency upon the dynamic performance of an attitude-angle control system, the following conclusions are reached.

For all autopilots considered, increasing the autopilot natural frequency causes the accuracy of control to improve, and the rise and response times to decrease. The improvement in the attitude-angle transient characteristics as the autopilot natural frequency increases is greater for changes in natural frequency from 30 to 70 radians per second with smaller improvement for natural frequencies greater than 70 radians per second for all flight conditions considered except at an altitude of 30,000 feet.

For all flight conditions considered, the required stored energy increases as the autopilot natural frequency increases from 30 to 70 radians per second. Beyond 70 radians, however, the amount of stored fluid necessary for control does not increase significantly for some flight conditions. The peak accumulator power does increase with increases in autopilot natural frequency. Also, the stresses in the missile's structure due to normal acceleration increases rapidly beyond a natural frequency of 70 radians per

second.

From the above considerations, an autopilot natural frequency of 70 radians per second appears to be a good compromise. At this frequency, the accuracy of control is sufficient, and the cost of constructing such an autopilot would not be excessive. Although it is possible to choose a higher natural frequency when the amount of stored energy or fluid is the only consideration, the peak power requirement and the missile's normal acceleration favor the lowest autopilot natural frequency that yields satisfactory control accuracy.

The data obtained from investigations of this type may be used by the control system designer in conjunction with space, weight, and economic considerations to determine the most practical automatic pilot specifications. For other missile configurations and control systems, a similar investigation would be required to obtain the data needed for selecting an autopilot compromise.

BIBLIOGRAPHY

BIBLIOGRAPHY

Bode, Hendrik W., Network Analysis and Feedback Amplifier Design. New York: D. Van Nostrand Company, Inc., 1950.

Brown, Gordon S., and Donald P. Campbell, Principles of Servomechanisms. New York: John Wiley and Sons, Inc., 1948.

Chestnut, Harold, and Robert W. Mayer, Servomechanisms and Regulating System Design. New York: John Wiley and Sons, Inc., Vol. I, 1951.

De Groff, Harold M., Ray C. Binder, John G. Truxal, and J. Robert Burnett, ''Fundamental Aspects of a Hydraulic-Type-Powered Flight-Control System,'' Aeronautical Engineering Review, 11:42-55, November, 1952.

Gardner, Murray F., and John L. Barnes, Transients in Linear Systems. New York: John Wiley and Sons, Inc., Vol. I, 1951.

Gardner, Robert A., and Jacob Zarovsky, Rocket-Powered Flight Test of a Roll-Stabilized Supersonic Missile Configuration. NACA RM L9K01a, 1950.

Gold, Harold, Edward W. Otto, and Victor L. Ransom, Dynamics of Mechanical Feedback-Type Hydraulic Servomotor under Inertia Load. NACA TN 2767, 1952.

Guillemin, E. A., The Mathematics of Circuit Analysis. New York: John Wiley and Sons, Inc., 1950.

Hall, Albert C., The Analysis and Synthesis of Linear Servomechanisms. Massachusetts: Technology Press, 1943.

Nelson, Walter C., and Anthony L. Passera, A Theoretical Investigation of the Influence of Auxiliary Damping in Pitch on the Dynamic Characteristics of a Proportionally Controlled Supersonic Canard Missile Configuration. NACA RM L50F30, 1950.

Seaberg, Ernest C., and Earl Smith, A Theoretical Investigation of an Automatic Control System with Primary Sensitivity to Normal Accelerations as Used to Control a Supersonic Missile Configuration. NACA RM L51D23, 1951.

Seamans, Robert C., Benjamin G. Bromberg, and L. E. Payne, "Application of the Performance Operator to Aircraft Automatic Control," Journal of Aeronautical Science, 15:535-55, September, 1948.

Tustin, A., Automatic and Manual Control. New York: Academic Press, Inc., 1952.

Wiener, N., Interpolation, Extrapolation, and Smoothing of Stationary Time Series. New York: John Wiley and Sons, Inc., 1948.

APPENDIX

APPENDIX A

LINEARIZATION OF THE TRANSFER VALVE CHARACTERISTICS YIELDING THE RESPONSE THAT THE SERVOMOTOR VELOCITY IS PROPORTIONAL TO THE VALVE DISPLACEMENT

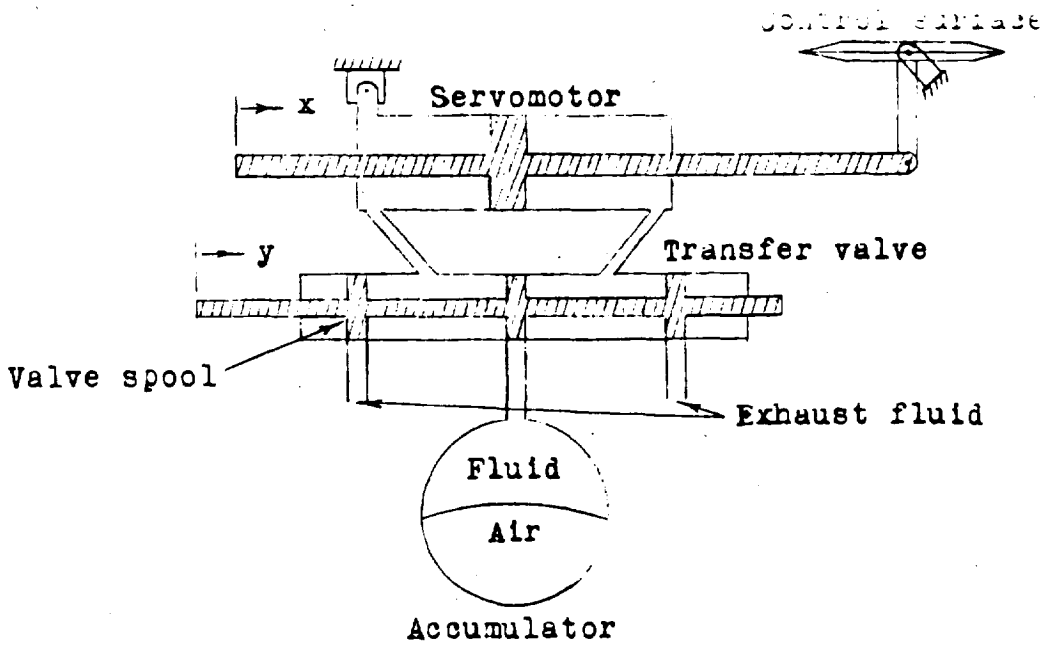

a area of the servomotor piston, inches^2

K_p proportionality constant between the volume rate of flow of fluid and the servomotor linear velocity, $\frac{q}{\dot{x}}$, feet^3/second per foot/second

K_v proportionality constant between the volume rate of flow of fluid and the transfer valve linear displacement, $\frac{q}{y}$, feet^3/second per foot

P pressure drop across the servomotor piston, pounds per inch^2

P_s pressure in the accumulator, $P + P_v$, pounds per inch^2

P_v pressure drop across the transfer valve, pounds per inch^2

q volume rate of flow of fluid, feet^3 per second

Z_c load impedance analagous to electrical impedance

The following is a plot of transfer valve flow characteristics which is representative of results obtained experimentally.

$P_{v3} > P_{v2} > P_{v1}$

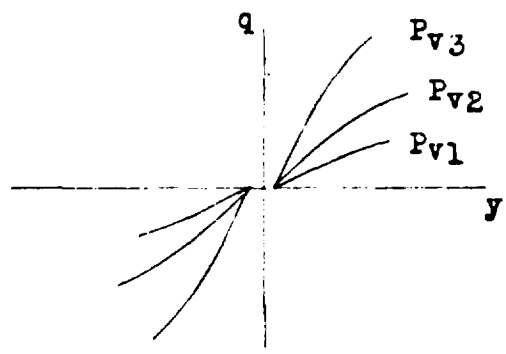

The dead spot shown at the origin is due to the valve spool overlapping the valve ports. If this characteristic is linearized by considering only small valve displacements--y--, no overlap, and small variations of the servomotor displacement--x--and all its derivatives, then

$$(1) \quad q = K_v y$$

Further, if the assumption of an incompressible fluid is made, the servomotor will satisfy the relation,

$$(2) \quad q = K_p \dot{x}$$

Therefore, if the accumulator pressure is of sufficient

magnitude such that

$$(3) \quad aP = Z_c\dot{x},$$

then from the relations, (1) and (2), the servomotor velocity is proportional to the valve displacement.

UNCLASSIFIED

APPENDIX B

LOG-MODULUS AND PHASE-ANGLE PLOTS AND NICHOLS CHARTS

Log-modulus and phase-angle plots--$\frac{\delta_A}{\epsilon_1}(j\omega)$, $\frac{\delta_r}{\theta_o}(j\omega)$, $\frac{\theta_o}{\delta}(j\omega)$, $\frac{G}{\theta_o}(j\omega)$--and Nichols charts with $\frac{\delta_r}{\delta}(j\omega)$ and $\frac{\theta_o}{\epsilon_1}(j\omega)$ plotted on the open-loop coordinates are illustrated for $M = 1.6$ at 4,000 feet and an autopilot natural frequency of 50 radians per second.

The Nichols chart, like the Nyquist diagram, indicates whether or not a system is stable and roughly indicates the amount of overshoot and response time to expect when the system is subjected to a step input signal. The superimposed contours yield the closed-loop response, $\frac{KG}{1 + KG}(j\omega)$, if $C = A - B$. $KG(j\omega)$ is the complex gain or response of a system's open-loop transfer function to sinusoidal inputs ($s = j\omega$).

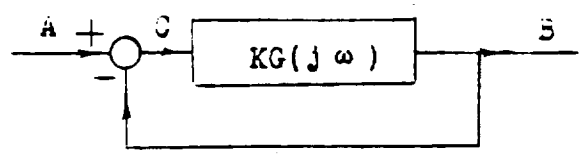

These methods are identical to those employed in network and feedback amplifier theory.

DECLASSIFIED

Log-Modulus and Phase-Angle Plot of $\frac{\delta_0}{\varepsilon}$ (ω)

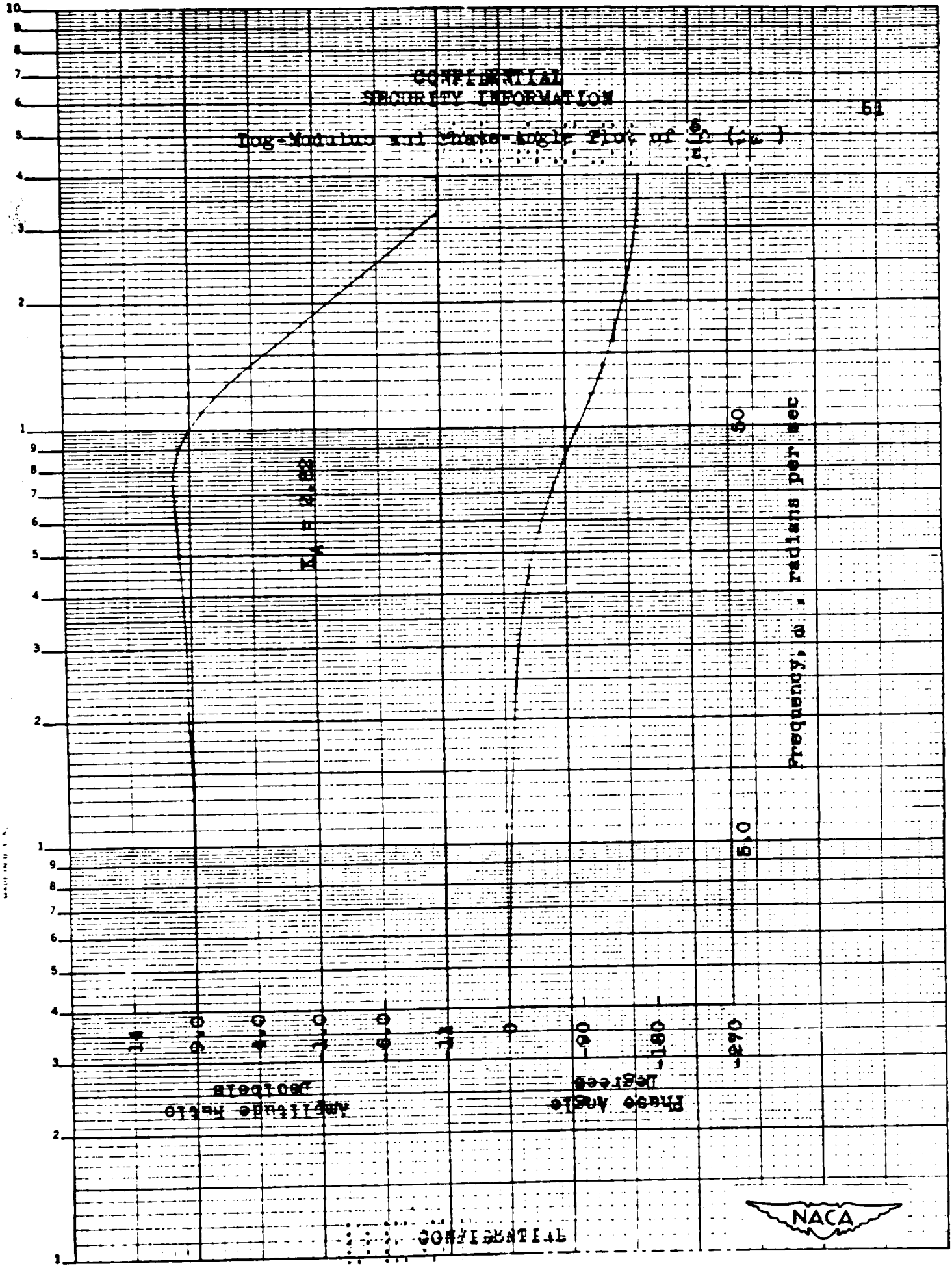

Log-Modulus and Phase-Angle Plot of $\frac{\phi}{\delta}(j\omega)$

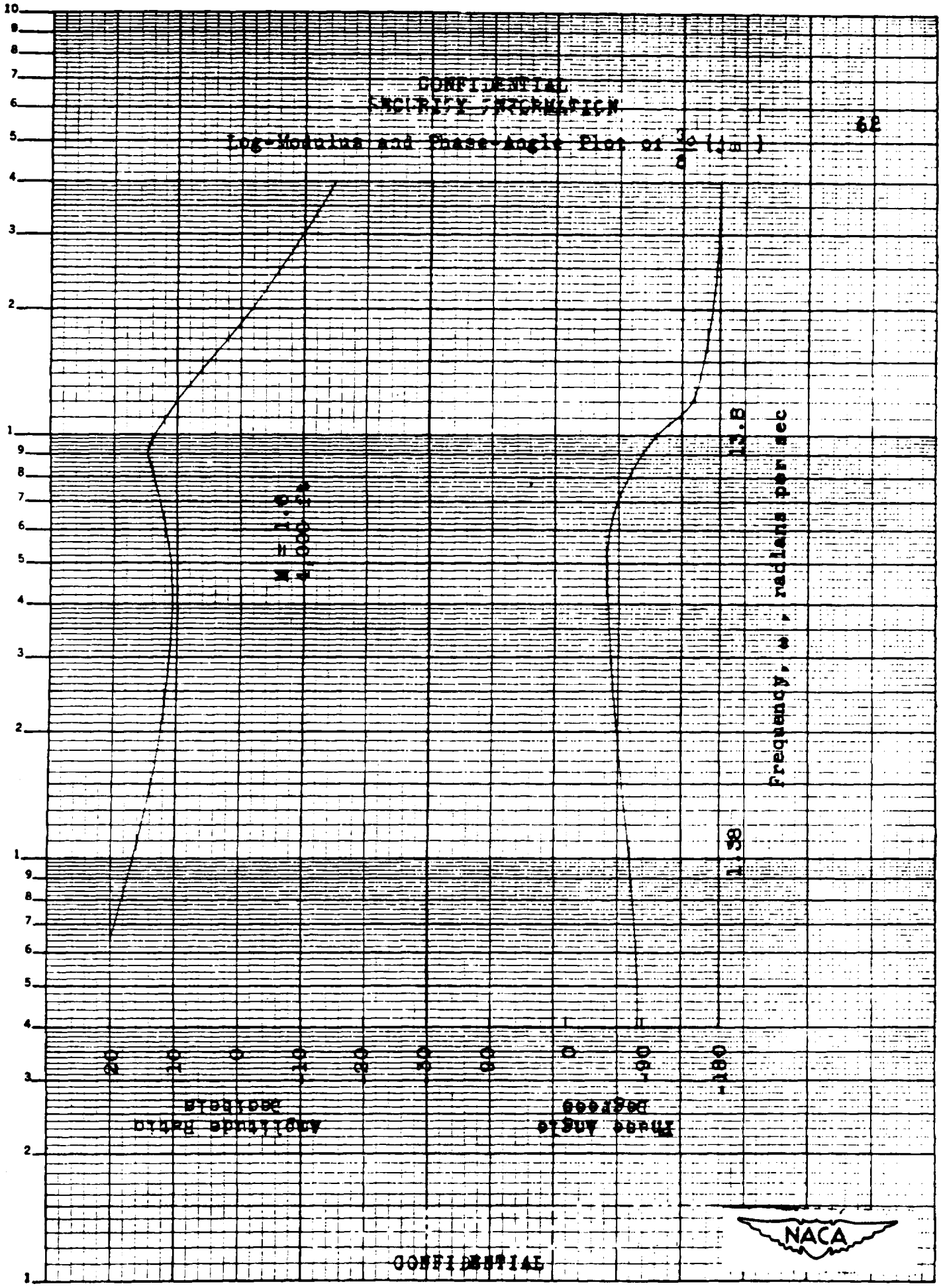

KEUFFEL & ESSER CO. N. Y. No. 359-710
Semi-Logarithmic, 3 cycles X 10 to the inch 5th line accented
MADE IN U.S.A.

Log-Modulus and Phase-Angle Plot of $\frac{\delta_J}{\delta_0}(j\omega)$
(Experimental Response)
$K_r = 1.0$

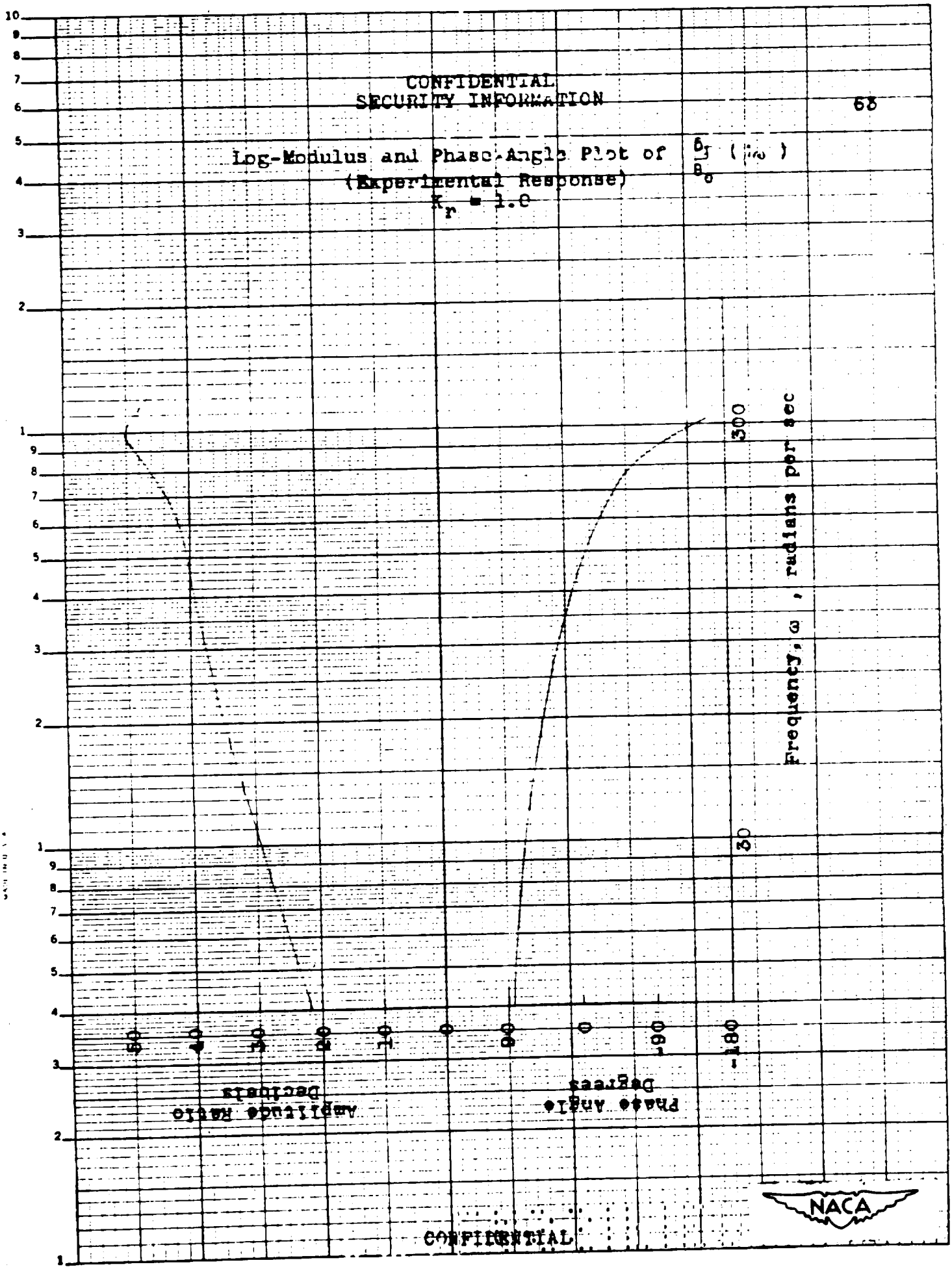

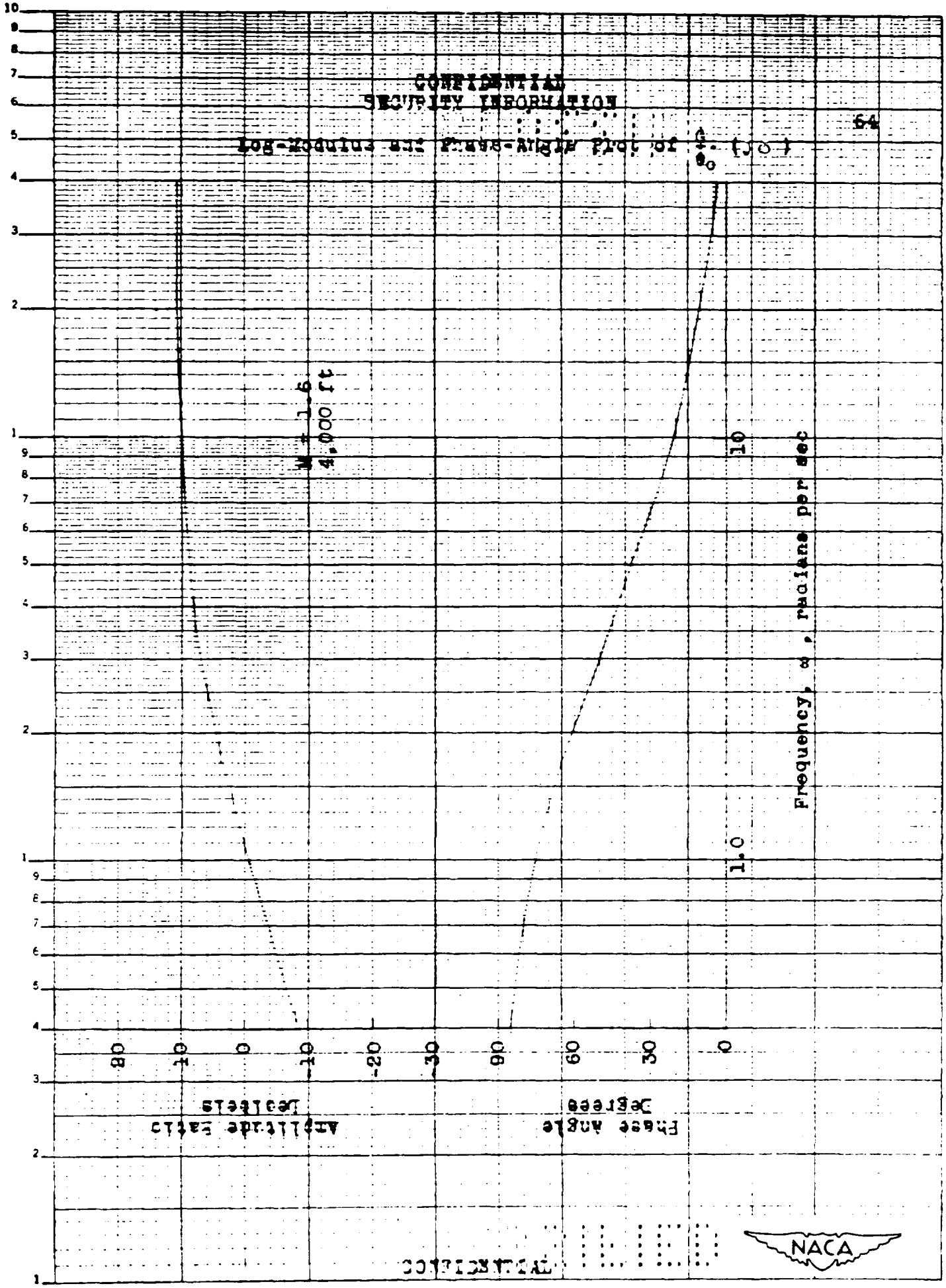
CONFIDENTIAL
SECURITY INFORMATION
Log-Modulus and Phase-Angle Plot of $\frac{G}{\theta_o}(j\omega)$
M = 1.6
4,000 ft
Frequency, ω, radians per sec
10
1.0
Amplitude Ratio
Decibels
Phase Angle
Degrees
80
10
0
-10
-20
-30
90
60
30
0
NACA
CONFIDENTIAL

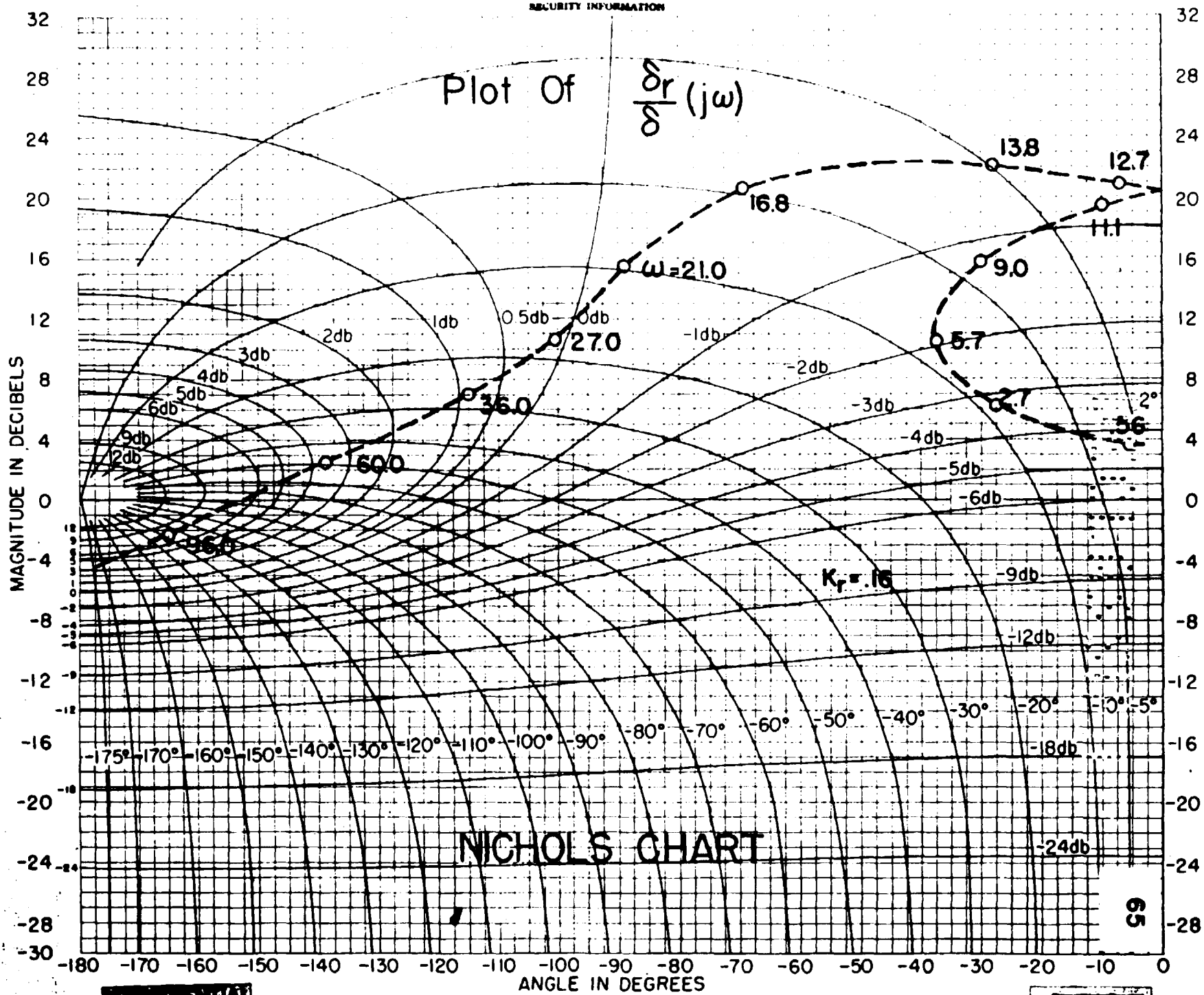
Plot Of $\frac{\delta_r}{\delta}(j\omega)$
NICHOLS CHART
MAGNITUDE IN DECIBELS
ANGLE IN DEGREES
$K_r = .16$
$\omega = 21.0$
13.8
12.7
16.8
11.1
9.0
5.7
2.7
.56
27.0
36.0
60.0
96.0
1db
0.5db
0db
-1db
-2db
-3db
-4db
-5db
-6db
-9db
-12db
-18db
-24db
2db
3db
4db
5db
6db
9db
12db
2°
-175°
-170°
-160°
-150°
-140°
-130°
-120°
-110°
-100°
-90°
-80°
-70°
-60°
-50°
-40°
-30°
-20°
-10°
-5°
32
28
24
20
16
12
8
4
0
-4
-8
-12
-16
-20
-24
-28
-30
-180
-170
-160
-150
-140
-130
-120
-110
-100
-90
-80
-70
-60
-50
-40
-30
-20
-10
0

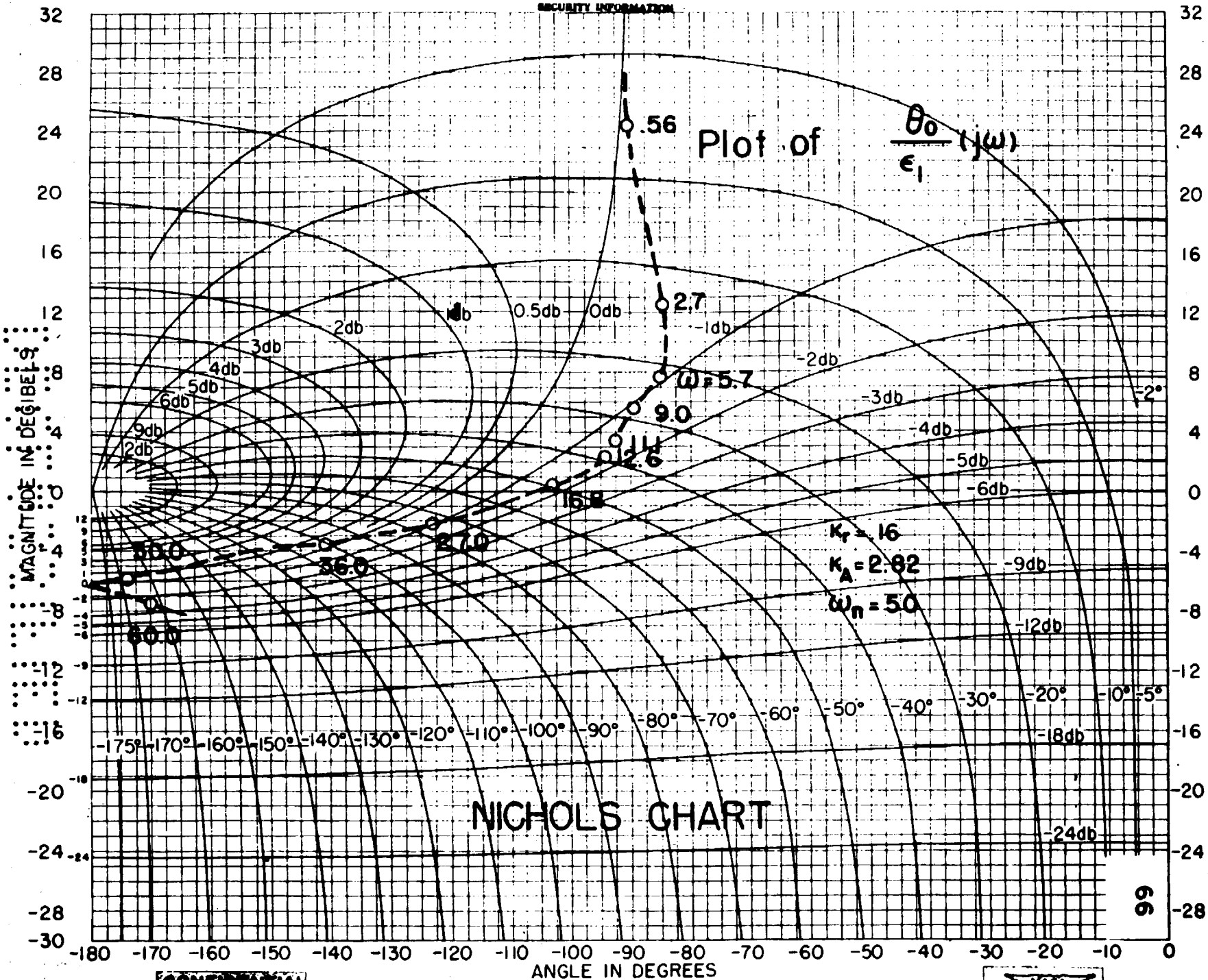
Plot of $\frac{\theta_o}{\epsilon_1}(j\omega)$
NICHOLS CHART
MAGNITUDE IN DECIBELS
ANGLE IN DEGREES
$K_T = .16$
$K_A = 2.82$
$\omega_n = 5.0$
$\omega = 5.7$
.56
2.7
9.0
12.6
15.8
27.0
36.0
50.0
60.0
0.5db
0db
-1db
-2db
-3db
-4db
-5db
-6db
-9db
-12db
-18db
-24db
2db
3db
4db
5db
6db
9db
12db
-2°
-5°
-10°
-20°
-30°
-40°
-50°
-60°
-70°
-80°
-90°
-100°
-110°
-120°
-130°
-140°
-150°
-160°
-170°
-175°
66